IEEE Access
Multidisciplinary | Rapid Review | Open Access Journal

Received August 2, 2021, accepted August 11, 2021, date of publication August 17, 2021, date of current version August 30, 2021.

Digital Object Identifier 10.1109/ACCESS.2021.3105515

A Fuzzy Sliding-Mode Control Based on Z-Numbers and LAMDA

L. MORALES[1], J. AGUILAR[2,3,4], (Member, IEEE), A. ROSALES[1], (Senior Member, IEEE), AND D. POZO-ESPIN[5]

[1]Departamento de Automatización y Control Industrial, Escuela Politécnica Nacional, Quito 170517, Ecuador
[2]CEMISID, Escuela de Ingeniería de Sistemas, Universidad de Los Andes (ULA), Mérida 5101, Venezuela
[3]GIDITIC, Universidad EAFIT, Medellín 050022, Colombia
[4]Departamento de Automática, Universidad de Alcalá, 28805 Alcalá de Henares, Spain
[5]Ingeniería en Electrónica y Automatización, Facultad de Ingeniería y Ciencias Aplicadas, Universidad de las Américas, Quito 170513, Ecuador

Corresponding author: D. Pozo-Espin (david.pozo@udla.edu.ec)

ABSTRACT Z-Numbers is a recent concept related to fuzzy logic where the restriction and reliability criteria are characterized as fuzzy sets. Due to the potential of Z-numbers, this paper presents the development of a fuzzy controller that combines the fundamentals of LAMDA (Learning Algorithm for Multivariate Data Analysis) with the concepts of the Total Utility of Z-numbers, to establish an inference method to improve the performance in a control system. The controller uses criteria from the sliding mode control (SMC) and the Lyapunov concepts to guarantee robustness and stability respectively. The LAMDA method is applied to compute a chattering-free control action which is applied to systems with model uncertainties and variable dynamics. The fuzzy controller has been tested by simulation in two different tasks: 1) Control of a process that consists of a mixing tank with variable dynamics, and 2) Trajectory tracking of a mobile robot. The proposed approach provides suitable results at runtime and outperforms the results of the other tested controllers in terms of performance, minimizing the deviation between the current system output and the reference. Finally, a complexity analysis is presented to evaluate the feasibility in the implementation of the proposal. The obtained results prove the suitability of using a LAMDA Z-number-based controller in the tested systems.

INDEX TERMS Intelligent control, LAMDA, Z-numbers, robustness, fuzzy control.

I. INTRODUCTION

Uncertain systems are characterized by inexact and fuzziness information, making their modeling and control difficult. The classical deterministic models used to control these systems are usually insufficient, which causes a decrease in the performance since they depend on the precise estimation of the parameters/variables of the models in their designs and calibration. The design of controllers and the modelling of its parameters to be implemented in systems (plants) with variable dynamics (industrial processes or robotic systems), are difficult due to the nonlinearities caused by vibrations, frictions and uncertain characteristics of the environment. These nonlinearities produce that the control system design has insufficient precision and limits the effectiveness of the controller. Several proposals have been developed in the literature to control systems with nonlinear characteristics in uncertain models. The most outstanding ones are the Sliding Mode Control (SMC) [1]–[4], the adaptive control [5], [6], the predictive control [7]–[9], nonlinear approaches [10]–[12], linear algebra approaches [13], [14], and intelligent approaches like neural network controllers [15]–[17] and fuzzy controllers [18]–[20], among others.

Nowadays, the use of machine learning strategies in the design of controllers has advanced considerably due to the improvements that they can bring to systems with uncertainties. For example, recent alternatives to the conventional Global Sliding Mode Control structure for an active power filter (APF) system are presented in [21], [22]. Its variants include a Recurring Feature Selection Neural Network (RFSNN) for learning an uncertain function, and a meta-cognitive fuzzy-neural-network (MCFNN) for dynamic tuning of membership functions, respectively. In both studies, the controller variants reach better performance and robustness.

The associate editor coordinating the review of this manuscript and approving it for publication was Shun-Feng Su.

Specifically, the Fuzzy Logic Control (FLC) has been applied in a large number of complex systems with good results and easy implementation. FLC presents a very good performance in plants in which the model is not exactly known [23]–[26], being a suitable method to design robust controllers capable, with satisfactory behavior against uncertainties [27]. The FLCs involve a set of heuristic rules to calculate the control output for the plant. For the rules-definition, expert knowledge about the system is required [28] to define the largest number of system operating conditions. The FLCs are considered within the group of intelligent controllers since they do not require an exact plant model. This artificial intelligence method has been used for many purposes in control theory, as plant modeling and control, scaling gains adaptation, system performance improvement, among others [29]. Lately, with the appearance of the Z-numbers, it is possible to develop fuzzy controllers that handle the constraint and reliability concepts, in order to improve the performance of the system by reducing the deviation between the reference and the current system output signal [30], [31].

Within fuzzy systems, the Learning Algorithm for Multivariable Data Analysis "LAMDA" [32] has been proposed. This method, originally designed to work in the classification and clustering context, has focused on the identification of functional states of a system. Several works have focused on the identification of the functional state using LAMDA as tool [33]–[37]. Initially, the algorithm computes the Marginal Adequacy Degree (MAD), a parameter that measures the contribution of the descriptors of an object to each cluster/class, with fuzzy probability functions like the Binomial or Gaussian functions [34]. Then, using fuzzy aggregation operators, the MADs in each class are combined to obtain as result the Global Adequacy Degree (GAD), a parameter that quantifies the membership degree of any individual to each class of the system [38]. Finally, LAMDA identifies and assigns the individual (object) to the most suitable class where the maximum GAD is computed [32], or in the case that the individual does not resemble a class enough, it is sent to the Non Informative Class (NIC).

Recently, we use the advantages of LAMDA to make it work in control systems, proposing an inference stage that uses the GADs to calculate the controller output. The class-based LAMDA controller has been validated in two different systems: the temperature regulation of a mixing tank [39], and in the regulation of humidity and temperature of a complex Heating, Ventilation, and Air-Conditioning (HVAC) system [40], presenting an excellent performance if we consider that the mathematical model of the plant is inexact or variable. In reference [41], we have proposed and formalized an Adaptive LAMDA for control and modeling of systems, modifying the LAMDA structure with the addition of layers operating similar to neural networks, but with the advantage of having a fixed number of layers whose calibration is not trivial. This method has a training phase to set initial values for the controller, and an application phase that consists of online learning to update the estimated model and compute the control action. This controller has proven to be adequate where the system dynamics are uncertain and complex [42]. Finally, our latest work [43] focuses on the formalization of a LAMDA algorithm for control based on the fundamentals of the Lyapunov theory and the Sliding-Mode Control (SMC), to guarantee stability and robustness of the overall system. The method is called LAMDA-SMC (LSMC) and takes advantage of LAMDA features to design a chattering-free controller. LSMC has been tested in the field of control of chemical processes, demonstrating that it is stable in the control of systems with model uncertainties.

On the other hand, Zadeh [44] has proposed the Z-numbers, an extension of the fuzzy numbers composed of two fuzzy elements: constraint and reliability. In a Z-number, the first component is used to characterize the uncertain information, and the second component is used to characterize the reliability (confidence) in the information. As it is analyzed in [31], the reliabilities of the fuzzy values of the variables in the set of rules are an issue in the modeling of the fuzzy systems, affecting the accuracy of the decision-making process. Taking into consideration the uncertainties in the process to be controlled, the concept of Z-number can be more effectively used for the design of control algorithms, which is the object of study of this paper.

A. RELATED WORKS

Currently, Z-numbers are studied in different application fields, such as: decision making, economics, optimization, risk assessment, prediction and rule-based systems characterization with imprecise information. Thus, one of the applications is in fuzzy reasoning to handle imperfect information characterized by the combination of fuzzy and probabilistic uncertainties in If-Then Rules systems [45]. The idea of converting a Z-number in a classic fuzzy number without losing information is rather significant for many applications. Kang *et al.* [46] present a proposal to solve this issue based on the Fuzzy Expectation of a fuzzy set, through a simple procedure that can be applied to triangular and trapezoidal membership functions, but remaining open to research the application in Gaussian functions.

Due to the novelty of working with Z, Aliev *et al.* [47] presents an initial proposal of basic operations that allow the treatment of uncertain information. Multi-Criteria Decision Making (MCDM) under uncertain environments has been studied in [48]–[51], in order to take into consideration efficiently the reliability information. Too, the conversion from a Z-number to a crisp number is useful in fuzzy decision-making and risk assessment. For this, [46] proposes to compute the centroid of the interval-valued of the fuzzy set with the Karnik-Mendel algorithm. Z-numbers also have been used for system state detection, especially failure modes in an aircraft turbine [52]. This paper demonstrates the viability of the proposed method using the reliability criterion. Finally, the Total Utility (TU) of a Z-number [53] is a new concept used to measure the total effects of a

Z-number, and can be used to determine the ordering of Z-numbers with the aim to be applied in MCMDs under uncertain environments. The advantage of this method is to be able to work with triangular, trapezoidal and Gaussian membership functions, considerably expanding its field of application, which could be used by LAMDA.

In control systems, there are few works that have focused their efforts on applying the concepts of Z-numbers in the design of controllers. Recently, Abiyev *et al.* [31], [54] presented a fuzzy inference system with Z-number for an omnidirectional robot. In these works, the fuzzy inference system is designed for controlling the angular and linear speeds of a robot soccer, independently. The proposed Z-rules are an extension of the classical fuzzy rules that consider the reliability of the constraint, but in all the rules is used the same reliability (Usually) to compute the control action. The inference method is based on distance measures of fuzzy sets, which takes the concepts of the α-cuts applied to the antecedent part, where the deviation of the input signals from the fuzzy values of the variables are determined. The proposed controller is tested and compared with other fuzzy methods, presenting interesting results. In [30], the same procedure is applied for a dynamic plant control where the response of the proposed controller is compared against the response of a conventional fuzzy controller, demonstrating the suitability of the controller in dynamic plants. Shalabi *et al.* [55] present the same procedure in the control of automotive air-spring suspension system where the technique is combined with genetic algorithms to estimate the optimal control gains and switching levels of the air volumes. Finally, the authors of [56] present the trajectory tracking of a wheeled robot, combining the reliability and constraint in multi-input/multi-output rules. The antecedent reflects the instantaneous distance measurements and the orientation gaps, and the consequent is obtained by interpolative reasoning and the graded mean integration method. The authors highlight that this approach avoids the complexity of encoding error gradients, and it is able to cope with missing observations.

B. CONTRIBUTION AND ORGANIZATION OF THE PAPER

The main motivation in this paper is the formalization of an LSMC controller based on Z-number (Z-LSMC) in order to reduce performance decay problems due to uncertainties in the modeling of the system. For this, we propose the use of the Total Utility of Z-numbers to obtain a more abrupt control action in the presence of large errors between the desired output and the reference, and smooth control actions as the error is minimized to improve the performance of the controller. This paper presents as the main contributions, the following:

- The development of a controller based on Z-numbers, whose inference mechanism is combined with the LAMDA fundamentals.
- The formalization of a controller that uses the class concept, considering the criteria of restriction and reliability, combined with the concept of Total Utility.
- The definition of Z-rules is based on different reliability values to modify the control action using the deviation between the system output and the desired reference, unlike works presented in [30], [31], [55], [56].
- The design of a fuzzy sliding-mode controller in which the control actions of the conventional SMC are calculated with the LAMDA method, in order to get a chattering-free controller.
- The controller stability analysis.
- A comparative performance analysis with previous results of the LSMC controller.

The Z-LSMC proposal is tested and validated by simulations in two continuous nonlinear systems: 1) regulation of a mixing tank with variable dynamics, and 2) trajectory tracking of a mobile robot, applying the controller to the dynamic part for the linear and angular velocity, independently.

This paper is structured as follows. In Section II is presented the background of LAMDA and a brief review of the Total Utility of Z-number. Section III defines the concepts used for the design of the Z-LSMC approach, such as the definition of the Z-rules of LAMDA and the reasoning process for the inference mechanism. Section IV presents the simulation results of the proposed algorithm using Matlab and VREP software. Finally, Section V describes the conclusions of this paper.

II. BACKGROUND

This section presents a brief description of the mathematical foundations to make LAMDA work as a controller as well as summarizes the Z-number theory used to improve the controller design.

A. LAMDA AS CONTROLLER

LAMDA is a classification/clustering algorithm that calculates the similitude measure between the descriptors that characterize a object $O = \left[o_1; \ldots; o_j; \ldots; o_l\right] \in \Re$, and the "$m$" classes $C = \{C_1; \ldots; C_k; \ldots; C_m\}$, to determine the class to which the object belongs. For that, LAMDA computes the Global Adequacy Degree (GAD).

In LAMDA, the descriptors are normalized $\bar{o}_j \in [0, 1]$, to operate in the same subspace. To normalize the descriptor o_j, it is required to know the maximum (o_{jmax}) and the minimum (o_{jmin}) values of the descriptor:

$$\bar{o}_j = \frac{o_j - o_{jmin}}{o_{jmax} - o_{jmin}} \tag{1}$$

Then, it is computed the MAD. The MAD determines the similitude of each descriptor of the object with the equivalent descriptor in a class k. The MADs are computed using probability density functions, e.g., the Gaussian [34]. In the case of the Gaussian function, it needs the average of the

descriptor j that belongs to the class k ($\rho_{k,j}$), defined as:

$$MAD_{k,j} = e^{-\frac{1}{2}\left(\frac{\bar{o}_j - \rho_{k,j}}{\sigma_{k,j}}\right)^2} \tag{2}$$

$$\rho_{k,j} = \frac{1}{n_{k,j}} \sum_{t=1}^{n_{k,j}} \bar{o}_j(t) \tag{3}$$

where $n_{k,j}$ and $\sigma_{k,j}$ are the number of elements and the standard deviation of the descriptor j in the class k, respectively. The parameter $\sigma_{k,j}$ is calculated as:

$$\sigma_{k,j}^2 = \frac{1}{n_{k,j} - 1} \sum_{t=1}^{n_{k,j}} (\bar{o}_j(t) - \rho_{k,j})^2 \tag{4}$$

The values $\rho_{k,j}$ and $\sigma_{k,j}$ are calculated during the training. Besides, a non-informative class NIC is generated with $\rho_{NIC,j} = 0.5$ and $\sigma_{NIC,j} = 0.25$. Objects not identified in any classes are sent to the NIC, which is the main LAMDA feature with respect to other algorithms.

Combining the MADs with fuzzy logic operators is computed the GAD. The GAD is a measure of the membership degree of the object O to each class k. The GADs are the product of linear interpolations of the S-norm and the T-norm, as the Dombi operator:

$$S(a, b) = 1 - \frac{1}{1 + \sqrt[p]{\left(\frac{a}{1-a}\right)^p + \left(\frac{b}{1-b}\right)^p}} \tag{5}$$

$$T(a, b) = \frac{1}{1 + \sqrt[p]{\left(\frac{1-a}{a}\right)^p + \left(\frac{1-b}{b}\right)^p}} \tag{6}$$

where $p \geq 1$ calibrates the sensitivity, and a, b are the MADs of the class k determined with the Dombi function.

The GAD of the normalized object $\bar{O}$ in each class k is obtained as:

$$\begin{aligned} GAD_{k,\bar{O}}&\left(MAD_{k,1}, \ldots MAD_{k,m}\right) \\ &= \delta T\left(MAD_{k,1}, \ldots, MAD_{k,m}\right) \\ &\quad + (1-\delta)\, S\left(MAD_{k,1}, \ldots, MAD_{k,m}\right) \end{aligned} \tag{7}$$

where $\delta \in [0, 1]$ is the exigency value. Values close to 1 make a stricter algorithm and values close to 0 make a permissive algorithm.

In the control context, LAMDA identifies the current state of the system and brings it to the desired state through the use of the GADs computed by (6). The desired state is where the error and its derivatives are equal to zero. For this purpose, it is required to define rules based on the system knowledge, concepts taken from the traditional FLCs. The expression that represents the fuzzy logic inference considering the LAMDA classes is:

$$\begin{aligned} Rule^{(k)}:\ IF\ o_1\ is\ F_1^p\ and\ \ldots o_j\ is\ F_j^q \ldots\ and\ o_l\ is\ F_l^r \\ THEN\ y_k\ is\ \gamma_k \end{aligned} \tag{8}$$

where o_j is the object descriptor taking values in the universe of discourse U_j. y_k takes values of the universe of discourse V. The fuzzy set $F_j = \left\{F_j^q : q = 1, 2, \ldots, Q\right\}$ belongs to U_j, the fuzzy set γ_k belongs to V, and $Rule^{(k)}$ is the rule applied to the class k.

The LAMDA inference mechanism uses the GADs of each class and the first order Takagi-Sugeno Kang (TSK) inference method [57]. In (8), γ_k is a singleton value specified for class k. Thus, the control output for LAMDA is computed as:

$$u = \Gamma \sum_{k=1}^{m} \gamma_k GAD_{k,\bar{O}} \tag{9}$$

$$\Gamma = \left| \frac{\text{argmax}\,(\gamma_k)}{\sum_{k=1}^{m} \gamma_k GAD_{k,\arg max(\bar{O})}} \right| \tag{10}$$

where u is the output of the controller, Γ is an adjustment parameter that works as a saturator and γ_k is the weight parameter applied in the class k.

The controller output of LAMDA depends on the weights γ_k applied to each GAD and depends on the centers $\rho_{k,j}$, which are established in the training stage (design). The LAMDA controller has a defined number of nodes that depend on the fuzzy sets (generally the same number "c") of each descriptor. The number of classes in LAMDA is $m = c^l$. Layer 1 has lc nodes, layer 2 has m nodes, and layer 3 has 1 node. The NIC is not used for the LAMDA controller because all the objects O are assigned to one predefined class.

B. Z-NUMBERS

A Z-number is a pair of fuzzy numbers defined as:

$$Z = \{(Az, Rz)\,|\mu_{Az} \epsilon\,[0, 1]\,,\ \mu_{Rz} \epsilon\,[0, 1]\} \tag{11}$$

where Az is the restriction (constraint) on the values of the observation x, and Rz is the reliability metric of the first fuzzy number in the space of y. For simplicity, Az and Rz are considered Gaussian fuzzy numbers defined by a binary (ρ, σ), where ρ is the center of the function and σ is the width of the function. E.g., Fig. 1 shows the membership functions of Az and Rz where it is appreciated how the parameters ρ, σ modify the position and shape of the curve, respectively.

A conventional fuzzy if-then rule presented in (8) for two inputs and one output can be stated as:

$$IF\ o_1\ is\ F_1^p\ and\ o_2\ is\ F_2^q\ THEN\ y_1\ is\ \gamma_1 \tag{12}$$

where F_1, F_2 are fuzzy sets and γ_1 is a singleton function.

In the case of Z-numbers, it is convenient to express a generalization of the basic if-then rule in terms of Z-valuations as follows:

$$\begin{aligned} IF\ o_1\ is\ \left(Az_1^p, Rz_1^p\right)\ and\ o_2\ is\ \left(Az_2^q, Rz_2^q\right) \\ THEN\ y_1\ is\ (\gamma_1, R_1) \end{aligned} \tag{13}$$

where Az_1^p, Rz_1^p, Az_2^q, Rz_2^q, are the fuzzy sets of the Z-number, γ_1 is the restriction, and R_1 is the reliability of the consequent for the Rule 1.

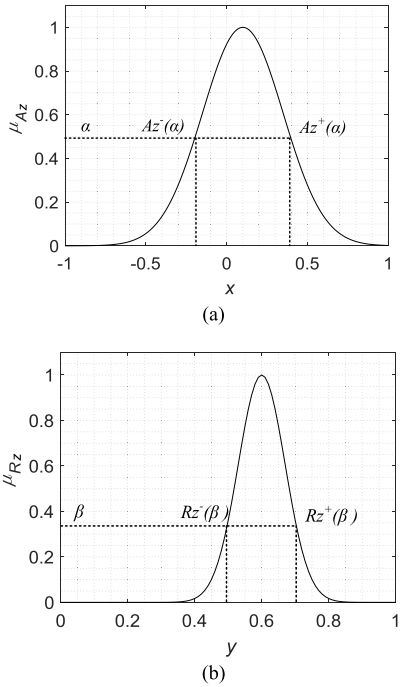

FIGURE 1. Membership functions of the Z-number $Z = (Az, Rz)$ with $Az = Gauss(0.1, 0.25)$, $Rz = Gauss(0.6, 0.07)$.

Some examples of the characterization of the Z-rules are:

- If the price of oil is likely high and the price of the refining process is commonly high, then the price of gasoline is very likely high.
- If the demand for luxury items is surely high, then consumers have very likely more purchasing power.

As seen in the examples, the application of Z-numbers is focused on modeling uncertain information from the real world. More examples of the real applications of Z-numbers are described in detail in [44]. In the case of control systems, there is a potential field of application of these concepts that we consider can improve the performance of the controller.

C. TOTAL UTILITY (TU)

The *TU* of Z-numbers is potentially useful to simplify the Z-number applications in fuzzy decision making tasks. The concept of *TU* is derived from the presentation of Z-numbers without subjective judgment as is stated in [53]. Such a simplification of the Z-numbers is of great importance when it is required to represent the restriction and the metric reliability in a single parameter, which can be useful in the design of intelligent controllers.

The procedure to compute is detailed as follows: let the mathematical expressions of the membership functions for Az and Rz defined as [53]:

$$\mu_{Az}(x) = e^{-\frac{1}{2}\left(\frac{x-\rho_1}{\sigma_1}\right)^2} \tag{14}$$

$$\mu_{Rz}(y) = e^{-\frac{1}{2}\left(\frac{x-\rho_2}{\sigma_2}\right)^2} \tag{15}$$

where $-1 \leq \rho_1 \leq 1$ is the center of the peak of the curve $\mu_{Az}(x)$, $\sigma_1 > 0$ is its standard deviation used to control the width of the bell, $0 \leq \rho_2 \leq 1$ is the position of the center of the peak of the curve $\mu_{Rz}(x)$, and $\sigma_2 > 0$ is its standard deviation.

If the α-cut, $\alpha = \mu_{Az}(x)$, then x is computed as:

$$x = \rho_1 \pm \sqrt{-2\sigma_1^2 ln\alpha};$$

$$Az^{\mp}(\alpha) = \rho_1 \mp \sqrt{-2\sigma_1^2 ln\alpha} \tag{16}$$

If the β-cut, $\beta = \mu_{Rz}(y)$, then y is computed as:

$$y = \rho_2 \pm \sqrt{-2\sigma_2^2 ln\beta};$$

$$Rz^{\mp}(\beta) = \rho_2 \mp \sqrt{-2\sigma_2^2 ln\beta} \tag{17}$$

The Total Utility of a Gaussian Z-number is computed as [53]:

$$TU(Z) = \int_0^1 \int_0^1 \int_{-1/2}^{1/2} \int_{-/22}^{1/2} \left[\frac{A_1}{2} + xA_2\right] e^{-A_2^2} \times \left[\frac{R_1}{2} + yR_2\right] e^{-\tilde{B}_2^2} d\delta \tag{18}$$

With $d\delta = dxdyd\alpha d\beta$ and:

$$A_1 = Az^{-}(\alpha) + Az^{+}(\alpha) \tag{19}$$

$$A_2 = Az^{+}(\alpha) - Az^{-}(\alpha) \tag{20}$$

$$R_1 = Rz^{-}(\beta) + Rz^{+}(\beta) \tag{21}$$

$$R_2 = Rz^{+}(\beta) - Rz^{-}(\beta) \tag{22}$$

Solving (18):

$$\begin{aligned} TU(Z) &= \int_0^1 \int_0^1 e^{-\tilde{A}_2^2} e^{-\tilde{B}_2^2} \int_{-\frac{1}{2}}^{\frac{1}{2}} \int_{-\frac{1}{2}}^{\frac{1}{2}} \left(\frac{A_1}{2}\frac{R_1}{2} + \frac{A_1R_2}{2}y + \frac{A_2R_1}{2}x + A_2R_2xy\right) dxdyd\alpha d\beta \\ &= \int_0^1 \int_0^1 e^{-A_2^2} e^{-R_2^2} \frac{A_1}{2}\frac{R_1}{2} d\alpha d\beta \\ &= \rho_1\rho_2 \int_0^1 \int_0^1 e^{-\left(2\sqrt{-2\sigma_1^2 ln\alpha}\right)^2} e^{-\left(2\sqrt{-2\sigma_1^2 ln\beta}\right)^2} d\alpha d\beta \\ &= \frac{\rho_1\rho_2}{\left(1+8\sigma_1^2\right)\left(1+8\sigma_2^2\right)} \end{aligned} \tag{23}$$

In some applications, the Z-numbers can be represented with the restriction and reliability of two singleton functions. In order to compute the TU of this kind of Z-numbers, we propose Theorem 1.

Theorem 1: The total utility of a fuzzy number with two singleton functions is equal to the product of the functions $TU(Z) \approx \rho_1\rho_2$.

Proof: According to (23), the *TU* is calculated based on the centers and variances of the two fuzzy numbers. From (14) and (15), if $\sigma_1 \approx 0$ and $\sigma_2 \approx 0$, then the Gaussian functions behave similarly to singleton functions (impulsive response in the centers ρ_1 and ρ_2), therefore:

$$TU(Z) = TU(Az, Rz) = \frac{\rho_1\rho_2}{\left(1+8\sigma_1^2\right)\left(1+8\sigma_2^2\right)} = \frac{\rho_1\rho_2}{\left(1+8\times0^2\right)\left(1+8\times0^2\right)} \approx \rho_1\rho_2 \tag{24}$$

D. EXTENSION OF LAMDA WITH Z-NUMBERS

The potential use of the Z-numbers combined with the concepts of TU has been detailed in Section II. Here, we consider its application with the LAMDA theory to design an intelligent controller.

As a starting point, we consider the Gaussian functions used to calculate MAD as presented in (2). This expression is similar to the one presented in (14). Therefore, the restriction in the case of LAMDA corresponds to MAD, thus $\mu_{Az} = MAD_{k,j}$. Also, it is necessary to measure the reliability parameter for μ_R, a procedure that will be detailed later in the document. If we have the two parameters of a Z-number, then it is feasible to compute the Total Utility of each class of the control system. LAMDA must identify the current state of the system to bring it to the desired state. For this purpose, it is necessary to define the rules for each class, similarly to the conventional FLCs. The systematic expression that generalizes (13) for the k-rule of the Z-fuzzy inference mechanism with LAMDA is denoted as:

$$Rule^{(k)}:\ IF\ o_1\ is\ Z_1^p\ and\ \ldots\ o_j\ is\ Z_j^q \ldots and\ o_l\ is\ Z_l^r \quad THEN\ y_k\ is\ Z^k \tag{25}$$

where o_j is the descriptor j of the object O. y_k belongs to the universe of discourse V. $Z_j^q = (A_j^q, R_j^q)$ denotes de Z-number for the descriptor j and the fuzzy set q, $Z^k = (\gamma_k, R_k)$ is the consequent Z-number, and $Rule^{(k)}$ is the rule for the class k.

In the context of LAMDA, we propose to use Z-number concepts to improve the controller response, thus rewriting (25) in terms of LAMDA for two inputs (descriptors) we have:

$$Rule^{(k)}:\ IF\ o_1\ is\ \left(MAD_{k,1}, \mu_{Rz1}\right)\ and\ o_2\ is\ \left(MAD_{k,2}, \mu_{Rz2}\right)\ THEN\ y_k\ is\ (\gamma_k, R_k) \tag{26}$$

The Total Utility is used to compute the new centers of the MADs and is used at the output to recalculate the weights applied to the GADs, making them adaptable as a function of the sliding surface s and $\dot{s}$, which are the descriptors of the proposed approach as detailed in section III.

III. Z-LSMC DESIGN

To design the Z-LSMC, it is considered an uncertain nonlinear continuous SISO (Single-Input Single Output) system with external bounded disturbances, as:

$$\begin{aligned} \dot{x}_i(t) &= x_{i+1}(t), \quad \forall n = 1, 2, \ldots, n-1 \\ \dot{x}_n(t) &= A(X,t) + b(X,t)\,u(t) + d(t) \end{aligned} \tag{27}$$

where: $X(t) = [x_1(t), \ldots, x_n(t)]^T = \left[x(t), \ldots, x^{(n-1)}(t)\right]^T \epsilon \Re^n$ is the state vector, the functions $A(X,t)$ and $b(X,t)$ are not exactly known nonlinear continuous and bounded. The control input is $u(t) \in \Re$, $d(t) \in \Re$ represents the disturbance $b(X,t)$ is a lower and upper bounded function such as $0 < b < |b(X,t)| < \bar{b}$.

$A(X,t)$ and $d(t)$ are supposed bounded:

$$|A(X,t)| \le \beta_A; \quad |d(t)| \le \beta_d \tag{28}$$

where the bounds β_A, β_d are positive.

The goal of a control system is to calculate a control law for $X(t)$ to track an n-dimensional desired trajectory $X_d(t) = [x_{d1}(t), \ldots, x_{dn}(t)]^T = \left[x_d(t), \ldots, x_d^{(n-1)}(t)\right]^T$, considering the external disturbances in the system and the model uncertainties.

The error is computed as:

$$\begin{aligned} E(t) &= X_d(t) - X(t) \\ &= [x_{d1}(t), \ldots, x_{dn}(t)]^T - [x_1(t), \ldots, x_n(t)]^T \\ &= [e_1(t), \ldots, e_n(t)]^T = \left[e(t), \ldots, e^{(n-1)}(t)\right]^T \end{aligned} \tag{29}$$

Thus, for any $X_d(t)$, the tracking error vector must satisfy the Euclidean norm:

$$\lim_{t\to\infty} \|E(t)\| = \|X_d(t) - X(t)\| = 0 \tag{30}$$

The SMC fundamentals establish to choose a continuous surface in order to the system can slide towards $X_d(t)$. In this work is used the surface proposed in [58]:

$$s(t) = \left(\frac{d}{dt} + \lambda\right)^n \int e(t)\,dt \tag{31}$$

where λ is a positive parameter.

We choose the sliding surface presented in (31), because, given the initial condition presented in (30), the problem of tracking $X_d(t) - X(t) = 0$ is equivalent to that of remaining on the surface $s(t)$ for all $t > 0$. Indeed, $s(t) = 0$ represents a linear differential equation whose unique solution is $e(t) = 0$, given initial conditions of (30). Thus, the problem of tracking the n-dimensional vector $X(t)$ can be reduced to that of keeping the scalar quantity $s(t)$ at zero, as shown below.

The advantage of the sliding surface, which as seen in (31) has an integral part, is that it helps to correct errors in the steady-state effectively without adding additional integrators to the controller output.

In Z-LSMC, LAMDA is used to calculate the control action (composed by the continuous and discontinuous part u_c and u_d, respectively) of conventional SMC through the procedure from (1)-(10).

Developing (31):

$$\begin{aligned} s(t) = \frac{d^{n-1}e(t)}{dt} + r_{n-1}\lambda\frac{d^{n-2}e(t)}{dt} + r_{n-2}\lambda^2\frac{d^{n-3}e(t)}{dt} \\ + \ldots + r_1\lambda^{n-1}e(t) + \lambda^n\int e(t)\,dt \end{aligned} \tag{32}$$

where $\{r_{n-1}, r_{n-2}, \ldots, r_1\}$ are the coefficients obtained by solving the polynomial presented in (31).

The first derivative of (32) is:

$$\begin{aligned} \dot{s}(t) &= e^{(n)}(t) + r_{n-1}\lambda e^{(n-1)} + \ldots + r_1\lambda^{n-1}\dot{e}(t) + \lambda^n e(t) \\ &= e^{(n)}(t) + \sum_{i=1}^{n} r_{n-i}\lambda^i e^{(n-i)} \end{aligned} \tag{33}$$

From (30), the n-derivative ($e^{(n)}(t)$) of the error is:

$$\begin{aligned} e^{(n)}(t) &= \dot{x}_{dn}(t) - \dot{x}_n(t) \\ &= \dot{x}_{dn}(t) - A(X,t) - b(X,t)\,u - d(t) \end{aligned} \tag{34}$$

As observed in (33) and (34), it is required to compute a control action u to satisfy $e^{(n)}(t) \rightarrow 0$. Based on the SMC fundamentals, u is composed of a discontinuous control action to move the states of the system to $s(t)$, and a continuous control action to retain the system on the selected surface [1]. The calculation of the continuous and discontinuous control actions is described below.

A. CONTINUOUS CONTROL ACTION

Considering the continuous control action as $u = u_c$, then replacing (34) in (33), it is obtained:

$$\dot{s}(t) = \dot{x}_{dn}(t) - A(X,t) - b(X,t)\,u_c - d(t) + \sum_{i=1}^{n} r_{n-i}\lambda^i e^{(n-i)} \quad (35)$$

Based on (35), it is required to compute u_c to fulfill $\dot{s}(t) = 0$, for this, it is necessary to identify the sign of $b(X,t)$ (or the gain of the system) linked to the input u_c to define the classes of LAMDA. Equation (35) shows that if $b(X,t) > 0$, then $\dot{s}(t)$ increases as u_c decreases, and vice-versa.

Five classes in the range of $[-1,1]$ for $\dot{s}(t)$ are defined, this supported by the scalability analysis that we performed in [43] where has been shown that selecting three or seven classes does not significantly affect the performance of controllers based on LAMDA, and the only required consideration is an adequate calibration of the scaling gains. The proposed classes for $\dot{s}(t)$ are: Positive Big ($PB = 1$), Positive Small ($PS = 0.5$), Zero ($ZE = 0$), Negative Small ($NS = -0.5$), and Negative Big ($NB = -1$). With these classes are defined the rules to obtain the normalized continuous control action u_{nc}. In order to calibrate the controller, the scaling gain k_1 is placed at the input $\dot{s}(t)$, and the scaling gain k_c at the output as:

$$u_c = k_c u_{nc} \Rightarrow$$
$$u_c = k_c ZLSMC(\dot{s}); \quad k_c > 0 \quad (36)$$

The rule table of u_c considering the value of $\dot{s}(t)$ as shown in (35) is presented in Table 1, considering $C_k = (\gamma_k, R_c); \forall k = \{1,2,\ldots,5\}$.

For the computation of the continuous control action, the classes per descriptor and the membership functions of the reliability are presented in Fig. 2. Note that for the reliability part the absolute value of $\dot{s}$ is used. In [31] is proposed the establishment of three classes to represent reliability in a simple and complete way for control systems. These are: "S" for "sometimes," "U" for "usually," and "A" for "always".

To define the rules in Table 1, when $b(X,t) > 0$, and based on (35), it is noted that $\dot{s}(t)$ decreases as u_c increases, and vice-versa. With this analysis are defined the rules in order to fulfill $\dot{s}(t) = 0$. For instance, if $\dot{s}(t)$ is NB, then a big negative (NB) u_c is required to increase rapidly $\dot{s}(t)$, and the reliability $|\dot{s}(t)|$ is assigned with a value sometimes "S" whose center is in 0.6. This causes the center calculated with the Total Utility to move to the left, which in fuzzy control means a more abrupt control action that causes a rapid decreasing of $\dot{s}(t)$.

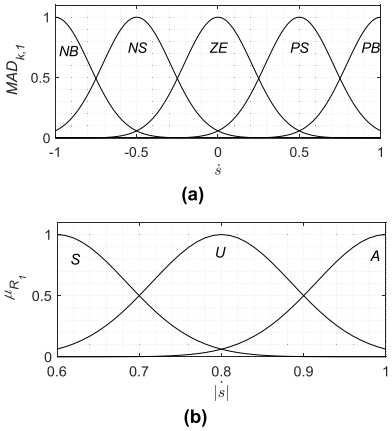

FIGURE 2. a) Membership functions for the MADs of $\dot{s}(t)$, b) reliability of $|\dot{s}(t)|$.

TABLE 1. Table of rules for the input $\dot{s}(t)$.

	$\dot{s}(t)$				
	NB,S	***NS,U***	***ZE,A***	***PS,U***	***PB,S***
$b(X,t) > 0$	$C_1 = NB, R_c$	$C_2 = NS, R_c$	$C_3 = ZE, R_c$	$C_4 = PS, R_c$	$C_5 = PB, R_c$
$b(X,t) < 0$	$C_1 = PB, R_c$	$C_2 = PS, R_c$	$C_3 = ZE, R_c$	$C_4 = NS, R_c$	$C_5 = NB, R_c$

If $\dot{s}(t)$ is NB, then the error and its derivatives are close to zero, which requires a small positive control action u_c to decrease slowly $\dot{s}(t)$. Also, in order to obtain a smoother control action, the reliability is assigned a value usually "U" whose center is in 0.8. Finally, if $\dot{s}(t) = 0$ ($\dot{s}(t) = $ ZE), then no control action is required because it is the desired condition. Thus, $u_c = ZE$ and the reliability is assigned a value always "A" whose center is in 1. Therefore, when $\dot{s}(t)$ is close to zero, then the control action is smoother.

As shown in Table 1, by using the value $|\dot{s}(t)|$, the same previous analysis is valid for the classes PB and PS.

On the other hand, when $b(X,t) < 0$ and based on (35), it is noted that $\dot{s}(t)$ decreases as u_c decreases, and $\dot{s}(t)$ increases as u_c increases. Therefore, as observed in Table 1, only the sign of the restriction changes and the criterion to define reliability is the same for the case $b(X,t) > 0$.

In the Z-LSMC, we only have two descriptors at the input of LAMDA, therefore, (2) is computed for s and its derivative, that is $j = 1$ for $\dot{s}$ and $j = 2$ for s. The calculation of the new class centers is made based on the $TU_{k,j}(Z)$ applied to the descriptor $\dot{s}$, replacing the LAMDA restriction and reliability in (23) to obtain:

$$TU\left(MAD_{k,1}, R_1\right) = \frac{\rho_{k,1} c_{R_1}}{\left(1 + 8\sigma_{k,1}^2\right)\left(1 + 8\sigma_{R_1}^2\right)} \quad (37)$$

where $R_1 = Gauss(c_{R_1}, \sigma_{R_1})$ is the reliability of the $MAD_{k,1}$.

Unlike works that address the control with Z-numbers [30], [31], [56], we do not define the reliability at the output, we compute its weight value as is proposed in [46]:

$$R_c = \frac{\int_0^1 |\dot{s}|\,\mu_{R1}(|\dot{s}|)}{\int_0^1 \mu_{R1}(|\dot{s}|)} \quad (38)$$

TABLE 2. Table of rules for the inputs $s(t)$ and $\dot{s}(t)$ with $b(X,t) > 0$.

		$\dot{s}(t)$				
		NB,S	NS,U	ZE,A	PS,U	PB,S
$s(t)$	PB,S	$C_5 = ZE, R_d$	$C_{10} = ZE, R_d$	$C_{15} = PS, R_d$	$C_{20} = PB, R_d$	$C_{25} = PB, R_d$
	PS,U	$C_4 = ZE, R_d$	$C_9 = ZE, R_d$	$C_{14} = PS, R_d$	$C_{19} = PB, R_d$	$C_{24} = PB, R_d$
	ZE,A	$C_3 = NB, R_d$	$C_8 = NS, R_d$	$C_{13} = ZE, R_d$	$C_{18} = PS, R_d$	$C_{23} = PB, R_d$
	NS,U	$C_2 = NB, R_d$	$C_7 = NB, R_d$	$C_{12} = NS, R_d$	$C_{17} = ZE, R_d$	$C_{22} = ZE, R_d$
	NB,S	$C_1 = NB, R_d$	$C_6 = NB, R_d$	$C_{11} = NS, R_d$	$C_{16} = ZE, R_d$	$C_{21} = ZE, R_d$

From (24), we use the weight of the reliability R_c and the singleton values γ_k. The Total Utility of the Z-number at the output can be denoted as:

$$\gamma_{R_c}^k = \gamma_k \times R_c \tag{39}$$

Then, the output of the control action u_{nc}, based on (9), (10) and (39), is computed as:

$$u_{nc} = \left| \frac{arg\,max\,(\gamma_k)}{\sum_{k=1}^{m} \gamma_k GAD_{k,max}(\bar{O})} \right| \sum_{k=1}^{m} \gamma_{R_c}^k GAD_{k,\bar{O}} \tag{40}$$

B. DISCONTINUOUS CONTROL ACTION

To compute u_d, the following Lyapunov function is selected:

$$V(s(t)) = \frac{1}{2} s(t)^2 \tag{41}$$

The first derivative of (41) is:

$$\dot{V}(s(t)) = s(t)\,\dot{s}(t) \tag{42}$$

To guarantee stability, Lyapunov theory establishes to satisfy the condition:

$$s(t)\dot{s}(t) < 0 \tag{43}$$

Replacing (35) in (43), considering only $u = u_d$:

$$s(t)\,\dot{s}(t) = s(t)\left(\dot{x}_{dn}(t) - A(X,t) - b(X,t)\,u_d - d(t) + \sum_{i=1}^{n} r_{n-i}\lambda^i e^{(n-i)} < 0\right) \tag{44}$$

Based on (44), to fulfill $s(t)\dot{s}(t) < 0$ is required to calculate u_d. Five classes are defined for the inputs $\dot{s}(t)$ and $s(t)$ based in the scalability analysis presented in [43], and three classes for the reliability as presented in [31]. Due to the normalization of the classes in a range of $[-1,1]$ is computed u_{nd}. Thus, the scaling gain k_2 is added at the input $s(t)$, and k_d at the output as:

$$\begin{aligned} u_d &= k_d u_{nd} \Longrightarrow \\ u_d &= k_d ZLSMC\,(s,\dot{s})\,; \quad k_d > 0 \end{aligned} \tag{45}$$

For the computation of the discontinuous control action based on Z-numbers, we address the case $b(X,t) > 0$ since in the opposite case ($b(X,t) < 0$), only the sign of the classes changes in the restriction part, as detailed in the definition of rules of Table 1. The centers of the Z-classes are presented in Table 2, considering $C_k = (\gamma_k, R_d)\,; \forall k = \{1, 2, \ldots, 25\}$.

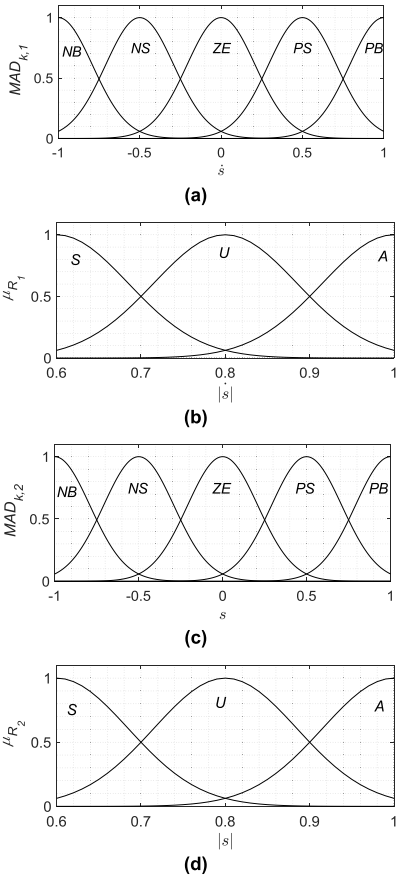

FIGURE 3. a) Membership functions for the MADs of $\dot{s}(t)$, b) reliability of $|\dot{s}(t)|$, c) Membership functions for the MADs of $s(t)$, d) reliability of $|s(t)|$.

For the discontinuous control action, the classes per descriptor and the membership functions of the reliability are presented in Fig. 3. Note that for the reliability part, the absolute values of $\dot{s}$ and s are measured, since we consider giving more weight when $|\dot{s}|$ and $|s|$ are far from zero.

In the Z-LSMC, for the discontinuous control action, we use the two descriptors at the input of LAMDA. Therefore, (2) is computed for s and its derivative, that is $j = 1$ for $\dot{s}$ and $j = 2$ for s. Then, the calculation of the new class centers is made based on the $TU_{k,j}(Z)$ as:

$$TU\left(MAD_{k,1}, R_1\right) = \frac{\rho_{k,1} c_{R_1}}{\left(1 + 8\sigma_{k,1}^2\right)\left(1 + 8\sigma_{R_1}^2\right)} \tag{46}$$

$$TU\left(MAD_{k,2}, R_2\right) = \frac{\rho_{k,2} c_{R_2}}{\left(1 + 8\sigma_{k,2}^2\right)\left(1 + 8\sigma_{R_2}^2\right)} \tag{47}$$

To compute the reliability at the output, we compute its weight value as is proposed in [46]:

$$R_d = arg\,max\left(\frac{\int_0^1 |\dot{s}|\,\mu_{R1(|\dot{s}|)}}{\int_0^1 \mu_{R1(|\dot{s}|)}}, \frac{\int_0^1 |s|\,\mu_{R2(|s|)}}{\int_0^1 \mu_{R2(|s|)}}\right) \quad (48)$$

It is proposed to choose the maximum value of the two reliabilities to obtain a more aggressive control action if the surface or its derivative are far from zero to take the system faster towards the reference.

To define the rules of Table 2, the following analysis has been considered:

- If $s(t)$ is positive and u_d decreases, then $s(t)\dot{s}(t)$ increases and vice-versa.
- If $s(t)$ is negative and u_d decreases, then $s(t)\dot{s}(t)$ decreases and vice-versa.

From the previous examination, it is proposed to compute the discontinuous control action u_d that guarantees $s(t)\dot{s}(t) < 0$. As has been described for u_c, the case of the discontinuous control action is similar, that is, S is associated as reliability to classes PB and NB, U to classes PS and NS and A to class ZE, in order to generate abrupt control actions when the surface and its derivative are far from the desired value, and smooth control actions when they are close to zero.

From (24), we use the weight of the reliability R_d and the values γ_k. The TU of the Z-number at the output can be denoted as:

$$\gamma_{R_d}^k = \gamma_k \times R_d \quad (49)$$

Then, the output of the control action u_{nd}, based on (9), (10) and (49), is calculated as:

$$u_{nd} = \left|\frac{arg\,max\,(\gamma_k)}{\sum_{k=1}^m \gamma_k GAD_{k,max(\bar{O})}}\right| \sum_{k=1}^m \gamma_{R_d}^k GAD_{k,\bar{O}} \quad (50)$$

As presented in (37)-(40) for the continuous control action and in (46)-(50) for the discontinuous control action, the application of Z-Numbers causes to obtain a control action that adapts to the characteristics of the sliding surface $s(t)$ and its derivative $s(t)$. This is achieved through the calculation of the Total Utility, which allows obtaining a more abrupt control action in the presence of large errors between the system output and the reference, and smooth control actions as the error is minimized and close to zero.

C. OVERALL CONTROL ACTION

Traditional SMC schemes such as the one proposed in [1], require the *sign* function to reach the sliding surface for the discontinuous action calculation. However, this function is smoothed through the addition of a parameter in the denominator δ, which removes robustness to the controller. In our scheme, using rules, we compute the discontinuous control action until reaching the sliding surface, as shown in (50), through the classes of LAMDA defined by its descriptors, which maintains robustness in the closed-loop. Thus, our method based on LAMDA avoids the utilization of the function "sign". Finally, the control action of Z- LSMC is calculated as:

$$u = k_c ZLSMC\,(\dot{s}) + k_d ZLSMC\,(s, \dot{s}) \quad (51)$$

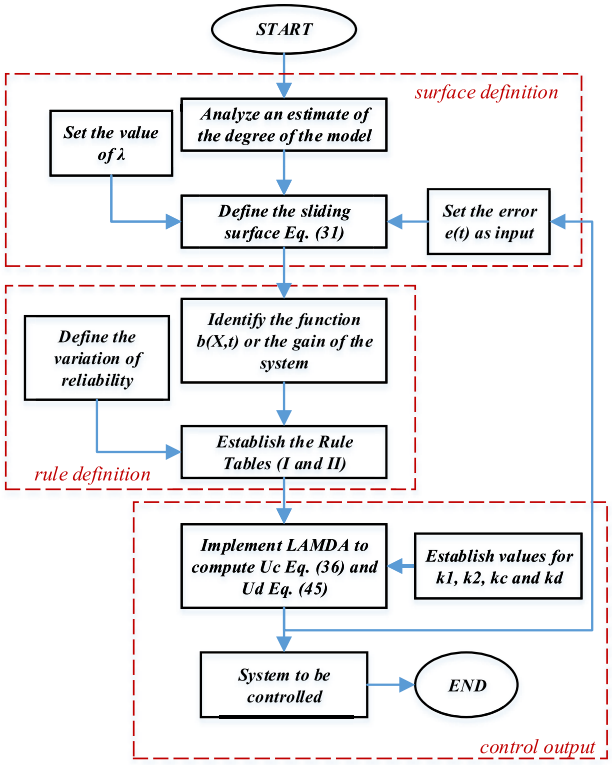

FIGURE 4. Flowchart for the design procedure of Z-LSMC.

The flow chart of the controller design is shown in Fig. 4, where the stages that allow the calculation of the control action are presented sequentially. The general steps (red highlighted boxes) in the scheme are a) the definition of the sliding surface, b) the definition of rules and, c) the calculation of the control action using LAMDA.

The Z-LSMC scheme is presented in Fig. 5, in which is observed: the blocks of the continuous ($ZLSMC_c(\dot{s})$) and discontinuous ($ZLSMC_d(s, \dot{s})$) outputs, the descriptors used, and the scaling gains.

D. STABILITY ANALYSIS

Considering the Lyapunov function in (41) and its first derivative presented in (42), the aim is to satisfy the condition $\dot{V} < 0$ [59]. Therefore, replacing (35) and (51) in (43) it is obtained:

$$\dot{V} = s\,(t)\left(\dot{x}_{dn}\,(t) - A\,(X,t) - b\,(X,t) \times (k_c ZLSMC\,(\dot{s}) + k_d ZLSMC\,(s,\dot{s})) - d\,(t) + \sum_{i=1}^{n} r_{n-i}\lambda^i e^{(n-i)}\right) < 0 \quad (52)$$

To demonstrate the stability of the Z-LSMC, the functions $A\,(X,t)$ and the disturbance $d(t)$ are supposed bounded as

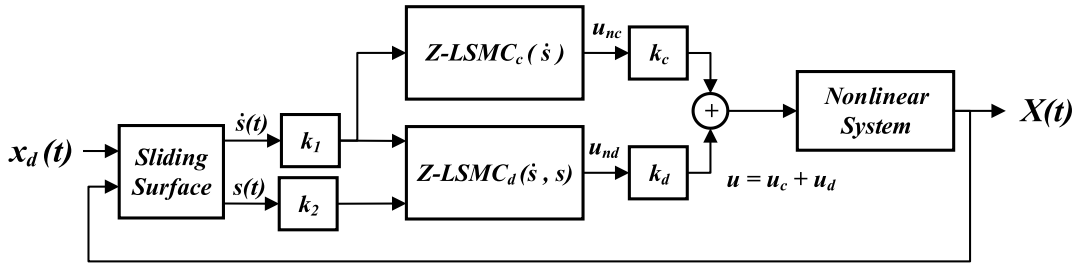

FIGURE 5. Block diagram of the Z-LSMC.

stated in (28). Also, the change of the reference $\dot{x}_{dn}(t)$ and the derivatives of the error $\sum_{i=1}^{n} r_{n-i}\lambda^i e^{(n-i)}$ must be assumed continuous and bounded [27]. Otherwise, they would be indeterminate and it would not be possible to guarantee the stability of the system.

$$|\dot{x}_{dn}(t)| \leq \beta_{dn}, \quad \left|\sum_{i=1}^{n} r_{n-i}\lambda^i e^{(n-i)}\right| \leq \beta_e \tag{53}$$

where β_{dn} and β_e are unknown positive constants.

Theorem 2: Considering the system of (27), with $u(t)$ as controller output defined in (51), and $(k_c + k_d) > \beta_{dn} + \beta_e - (\beta_d + \beta_A)$, then the error vector converges to the sliding surface.

Assuming for simplicity $b(X,t) = 1$, without loss of generality for systems in which $b(X,t) > 0$ (because our controller only requires to know the sign of the function $b(X,t)$), from [28] and Table 2, it is demonstrated that $k_d u_d = k_d|s|$ and $k_c u_c = k_c|s|$. Thus, replacing the inequalities (28) and (53) in (52):

$$\begin{aligned}\dot{V} &= s\Big(\dot{x}_{dn}(t) - A(X,t) - k_c ZLSMC(\dot{s}) \\ &\quad - k_d ZLSMC(s,\dot{s}) - d(t) \\ &\quad + \sum_{i=1}^{n} r_{n-i}\lambda^i e^{(n-i)}\Big) \\ &\leq \beta_{dn}|s| - \beta_A|s| - k_c|s| - k_d|s| - \beta_d|s| + \beta_e|s| \qquad (54)\\ \dot{V} &\leq \beta_{dn}|s| - \beta_A|s| - k_c|s| - k_d|s| - \beta_d|s| + \beta_e|s| \\ &= \left[-(k_c + k_d) + (\beta_{dn} + \beta_e - \beta_d - \beta_A)\right]|s| \qquad (55)\end{aligned}$$

Therefore, if the scaling gains are $(k_c + k_d) > \beta_{dn} + \beta_e - (\beta_d + \beta_A)$, then it is concluded that the reaching condition $s(t)\dot{s}(t) < 0$ is always fulfilled. Therefore, the proof is completed. The theorem is valid if $b(X,t) < 0$, as detailed in [43].

As a summary of the Z-LSMC design, the following steps are identified:

- Estimate the system order for the sliding surface of (31)
- Recognize the sign of $b(X,t)$.
- If $b(X,t) > 0$, then use Table 1 to compute u_c with the procedure from (36)-(40), and use Table 2 to compute u_d with the procedure from (45)-(50).
- If $b(X,t) < 0$, then use Table 1 and change the sign of the restriction (first parameter of the Z-number) in the consequent of Table 2.
- Calibrate the scaling gains of Z-LSMC.

The Z-LSMC scaling gains (k_1, k_2, k_c, k_d) have not a formalized equations for proper calibration, and we will consider its mathematical formalization in a future work. However, the parameter λ can be calibrated with the method presented in [1]. For the scaling gains calibration, this work uses the heuristic method, based on trial and error. This tuning procedure is one where general rules are followed to obtain approximate or qualitative results according to the system requirements [28]. The Z-LSMC controller has been calibrated based on the measurement and reduction of the Integral Square Error "ISE". This index is used because it integrates the square of the error over time, penalizing large errors more than smaller ones. Therefore, the controller that obtains the minimum index performs the best.

IV. SIMULATIONS AND RESULTS

The Z-LSMC is validated and tested in two different SISO nonlinear continuous systems: A. Regulation of a mixing tank with variable dynamics, a process in which it is required to work on a desired operating point maintaining the fixed reference. Being a system with high non-linearity due to the variation of its parameters, it is an ideal case to apply disturbances that change the output of the system, allowing us to evaluate the ability of the controller to bring the system towards the reference. B. Trajectory tracking of a mobile robot, this case only focuses on evaluating the performance of the controller when the trajectory changes smoothly and abruptly, for which several trajectories are established. It should be noted that for the design of the controllers, the same number of membership functions (classes) is maintained in both simulations. However, the rules change for $b(X,t) < 0$ and $b(X,t) > 0$. Five rules have been established per descriptor (detailed in sections III.1 and III.2) for the two simulations since, based on the sensitivity analysis presented in [43], a good response of the controller is observed without excessive computational load. Finally, the prior gains (k_1, k_2, k_c, k_d) are tuned through a heuristic calibration.

Finally, the results are validated through comparisons with the PID, SMC [1], LAMDA-PID [40], and the LSMC

controller [43]. LAMDA-PID and LSMC are recent controllers, which serve as the basis for the design of the Z-LSMC proposal. The PID controller has been considered because it is the best known worldwide, capable of controlling a large number of systems in real applications, which is why it is interesting to observe its performance in systems with variable dynamics. The SMC has been considered because it is a controller with robust characteristics with very good behavior in systems with variable dynamics and whose theoretical foundations are also used in the context of the design of the Z-LSMC proposal.

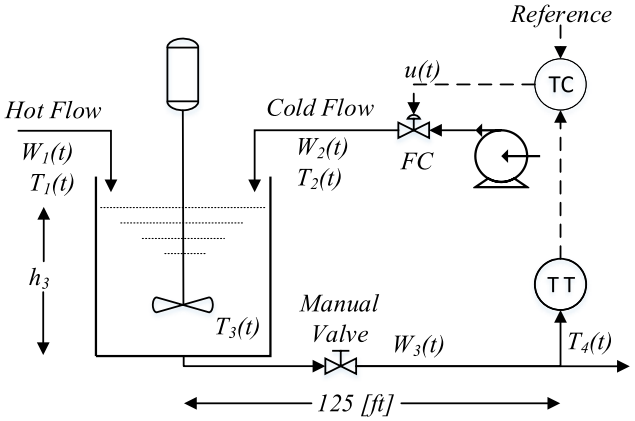

FIGURE 6. Scheme of the process with the mixing tank.

A. CASE STUDY 1: MIXING TANK PROCESS

This system consists of the mixture of two liquids in a tank as shown in Fig. 6. The volume of the tank varies freely without overflowing. In the tank are mixed a hot water stream $W_1(t)$ with a cold water stream $W_2(t)$, which is controlled with a valve. At the outlet of the tank, the mixture is transported by a water stream $W_3(t)$, which is required at the desired temperature. At a distance of $L = 125[ft]$ from the tank outlet, is installed a temperature transmitter, which operates between $100[°F]$ and $200[°F]$. The pipe length L generates a time delay (dead time) in the measurement.

For the system analysis, the following considerations are accepted:

- The tank output and the pipe are insulated.
- The liquid inside the tank varies and does not overflow.
- The liquids inside the tank are well mixed.
- The foremost disturbance is $W_1(t)$.

The approximate modelling of the mixing tank is described by the following dynamics:

- Manual actuator (valve)

$$W_3(t) = 11.8685 C_{VL3} \sqrt{h_3(t)} \tag{56}$$

- Mass balance of the liquids inside the tank:

$$W_1(t) + W_2(t) - W_3(t) = A_3 \frac{dh_3(t)}{dt} \tag{57}$$

TABLE 3. Steady-state values at the operating point of the process.

Variable	Value	Variable	Value
W_1	$250\ lb/min$	h_3	$4.26509\ ft$
W_2	$191.17\ lb/min$	C_{VL3}	$18\ gpm/ft^{1/2}$
W_3	$441.17\ lb/min$	C_{VL}	$gpm/psi^{1/2}$
Cp_1	$0.8\ Btu/lb - °F$	TO	$0.5\ p.u.$
Cp_2	$1.0\ Btu/lb - °F$	V_p	0.478
Cv_3	$0.9\ Btu/lb - °F$	ΔP_v	$16\ psi$
Cp_3	$0.9\ Btu/lb - °F$	u	$0.478\ p.u.$
T_1	$250\ °F$	A_3	$3.51692\ ft^2$
T_2	$50\ °F$	A	$0.2006\ ft^2$
T_3	$150\ °F$	G_f	1
ϱ	$62.4\ lb/ft^3$		

- Energy balance of the liquids inside the tank:

$$W_1(t)\,Cp_1 T_1(t) + W_2(t)\,Cp_2 T_2(t) - W_3(t)\,Cp_3 T_3(t) = A_3 Cv_3 \frac{d\left(h_3(t)\,T_3(t)\right)}{dt} \tag{58}$$

- Pipe delay

$$T_4(t) = T_3(t)\,(t - t_0(t)) \tag{59}$$

- Time delay of the system (dead time)

$$t_0(t) = \frac{LA\varrho}{W_3(t)} (60) \tag{60}$$

- Temperature transmitter

$$\frac{dTO(t)}{dt} = \frac{1}{\tau_T}\left[\frac{T_4(t) - 100}{100} - TO(t)\right] \tag{61}$$

- Dynamics of the control valve:

$$\frac{dV_p(t)}{dt} = \frac{1}{\tau_{V_p}}\left[u(t) - V_p(t)\right] \tag{62}$$

- Valve dynamics

$$W_2(t) = \frac{500}{60} C_{VL} V_p(t) \sqrt{G_f \Delta P_v} \tag{63}$$

The nomenclature presented from (56)-(63) in corresponds to C_p: liquid heat capacity, $[Btu/lb - °\mathrm{F}]$, C_v: liquid heat capacity $[Btu/lb - °\mathrm{F}]$, h_3: tank content level $[ft]$, A: mixing tank cross-section $\left[ft^2\right]$, $T_1(t)$: hot flow temperature $[°F]$, $T_2(t)$: cold flow temperature $[°F]$, $T_3(t)$: liquid temperature inside the tank $[°F]$, $T_4(t)$: temperature $T_3(t)$ considering the delay $t_0\,[°F]$, t_0: dead time $[min]$, ϱ: density of the contents of the mixing tank $\left[lb/ft^3\right]$, C_{VL}: valve flow coefficient $\left[gpm/psi^{1/2}\right]$, $TO(t)$: transmitter output signal from 0 a 1 $[p.u]$, $V_p(t)$: valve position 0 (closed), 1 (open), $u(t)$: the fraction of controller output (0 to 1) $[p.u]$, G_f: specific gravity, ΔP_v: pressure drop across the valve $[psi]$, τ_T: temperature sensor time constant $[min]$, τ_{V_p}: control valve time constant $[min]$, A: pipe cross-section $\left[ft^2\right]$. Table 3 details the parameters of the system in steady-state at the required operating point.

Camacho and Smith [1] propose to model this nonlinear chemical processes with an approximation of a first-order-plus dead time (FOPDT) system. Following the procedure presented in [60], as an example are observed the changes

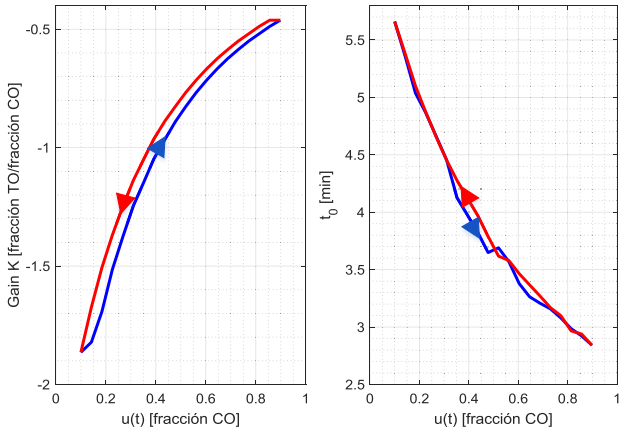

FIGURE 7. K and t_0 variations as function of the control action $u(t)$.

of the characteristic parameters (K, and t_0,) varying the signal $u(t)$ applied to the actuator that controls $W_2(t)$ in successive step changes as shown Fig.7. Here, it is observed that the dynamics of the plant vary ascending (blue) and descending (red) over the entire range of $u(t)$. This characteristic increases the nonlinearity of the system, which makes the modeling difficult for the design and calibration of a conventional model-based controller.

The Z-LSMC controller design is based on the procedure in subsection II.D. At the operation point, the system has been approximated to a FOPDT, as presented in [1]:

$$\frac{X(s)}{U(s)} = \frac{Ke^{-tos}}{\tau s + 1} \tag{64}$$

For example, the parameter identification for $u(t) = 0.478$ gives the characteristic values: $=-0.89$, $\tau = 0.92min$, $t_0 = 3.65min$.

Modeling t_0 using a first-order Taylor series approximation [1] is:

$$e^{-tos} \cong \frac{1}{t_0 s + 1} \tag{65}$$

Replacing (65) in (64):

$$\frac{X(s)}{U(s)} \cong \frac{K}{(\tau s + 1)(t_0 s + 1)} = \frac{K}{\tau t_0 s^2 + (\tau + t_0) s + 1} \tag{66}$$

Solving (66) in the time domain:

$$\tau t_0 \ddot{x} + (\tau + t_0)\dot{x} + x - Ku = 0 \tag{67}$$

The system model in state-space, where $x_1 = x$, is:

$$\begin{aligned} \dot{x}_1 &= x_2 \\ \dot{x}_2 &= -\frac{(\tau + t_0)}{\tau t_0} x_2 - \frac{1}{\tau t_0} x_1 + \frac{K}{\tau t_0} u \end{aligned} \tag{68}$$

From (68) it is a second-order system ($n = 2$). Thus, from (31), $s(t)$ is:

$$\begin{aligned} s(t) &= \left(\frac{d}{dt} + \lambda\right)^2 \int e(t)\, dt \\ &= \dot{e}(t) + 2\lambda e(t) + \lambda^2 \int e(t)\, dt \end{aligned} \tag{69}$$

The first derivative of (69) is:

$$\dot{s}(t) = \ddot{e}(t) + 2\lambda \dot{e}(t) + \lambda^2 e(t) = 0 \tag{70}$$

For $n = 2$ in (29):

$$\ddot{e}(t) = \dot{x}_{d2}(t) - \dot{x}_2(t) \tag{71}$$

Substituting (68) and (71) in (70):

$$\begin{aligned} \dot{s}(t) = \dot{x}_{d2}(t) + \frac{(\tau + t_0)}{\tau t_0} x_2 + \frac{1}{\tau t_0} x_1 - \frac{K}{\tau t_0} u + 2\lambda \dot{e}(t) \\ + \lambda^2 e(t) = 0 \end{aligned} \tag{72}$$

Fig. 7 shows that the gain of the process is negative $K < 0$ for the complete range of $u(t)$, so, $b(X, t) < 0$. The rule tables change the sign of the consequent restriction (first parameter) with respect to Tables 1 and 2, as stated in the fourth point of the summary for the design procedure of the Z-LSMC. Figs. 8 and 9 present the implemented rules for the continuous and discontinuous control actions for the mixing tank.

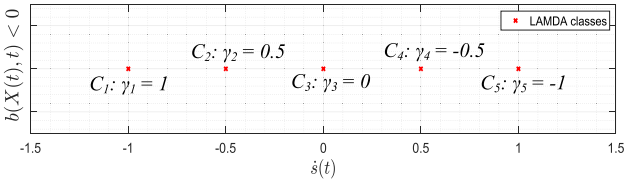

FIGURE 8. Classes and rules for u_c based on $\dot{s}(t)$ for the mixing tank.

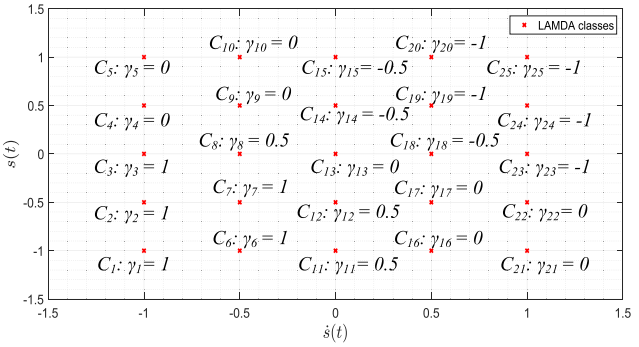

FIGURE 9. Classes and rules for u_d based on $\dot{s}(t)$ and $s(t)$ for the mixing tank.

To validate the Z-LSMC, different controllers are tested in this case study. A PID, SMC [1], LAMDA-PID Reference [56] recommends the design of a PID when $t_0 > \tau/4$. The controller parameters have been calibrated considering the method of Dahlin synthesis, obtaining $K_C = -0.17$, $\tau_I = 1$ and $\tau_D = 1.7$. The SMC has been tuned by the procedure in [1], these are: $\lambda_0 = 0.60$, $\lambda_1 = 1.55$, $K_D = 0.25$, $\delta = 0.71$. All the LAMDA proposals have been calibrated empirically with the ISE (Integral Square Error) minimization criterion. LAMDA-PID has been tuned with the parameters $k_p = 0.25$, $k_i = 0.4$, $k_d = 2.5\times10^{-5}$, the LSMC and Z-LSMC have the parameters $\lambda = 1$, $k_1 = 2.5 \times 10^{-5}$, $k_2 = 0.25$, $k_c = 5$ and $k_d = 0.58$. For these last two controllers, the parameters are the same to make a just comparison.

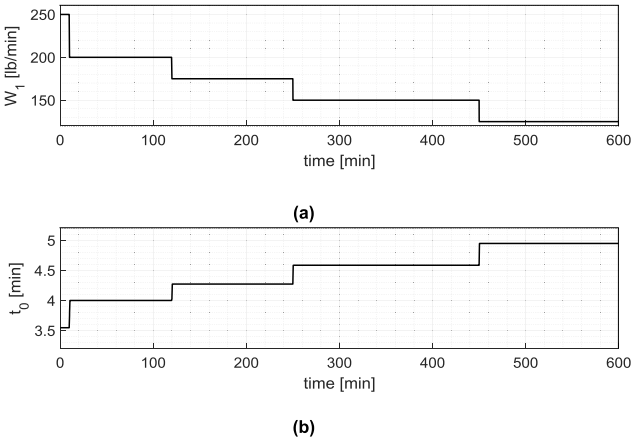

FIGURE 10. (a) Change of W_1, (b) change of dead time t_0.

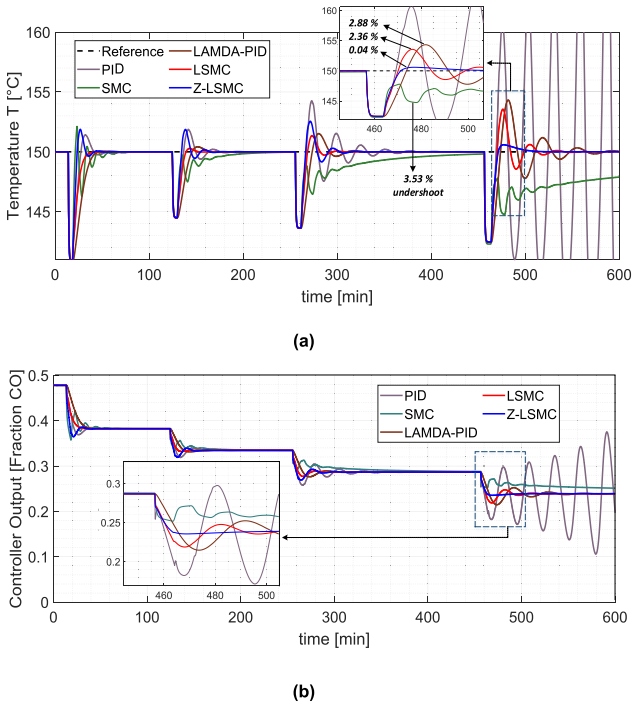

FIGURE 11. (a) Comparative desired temperature T, (b) control actions.

The change of W_1 (see Fig. 10a) is considered as the disturbance of the system. It varies from 250[lb/min] to 125[lb/min] in different time periods. The change W_1 affects the dynamics of the process. Fig. 10b shows the behavior of t_0 produced by the changes of W_1 in the open-loop system.

The controllers SMC, PID, LAMDA-PID, LSMC, and Z-LSMC, to regulate the mixing tank considering the disturbances presented in Fig. 9a are simulated in the software Matlab (Simulink). Fig. 11a shows the temperature outlet of the system, and Fig. 11b presents the control actions obtained by each proposal in order to make a qualitative analysis of the results.

Fig. 10a shows that Z-LSMC controls the desired temperature effectively in the shorter time, with a small overshoot, especially when W_1 decreases to 125[lb/min], while the controllers LSMC and LAMDA-PID are stable but oscillatory, the PID is unstable, and the SMC does not reach the reference during the simulation time.

It is observed that Z-LSMC presents an interesting behavior with respect to the other proposals, since in the disturbance at $t = 450$ min, the algorithm is able to reach the reference quickly with a minimum overshot compared to LSMC. These proposals present the best responses in the regulation task; however, it can be noted that Z-LSMC improves, even more, the performance of the LSMC controller as shown in the zoom of Fig. 11. The images present in detail the temperature outlet and the control actions for the last disturbance, in which it is observed that the overshot of Z-LSMC (0.04%) is much lower than that of Z-LSMC (2.36%), which is a great advantage since the actuator will consume less energy to reach the reference.

The LAMDA-PID regulates the process effectively with a moderate presence of oscillations for the last disturbance, but it is robust enough to keep the system stable. The SMC reaches the reference for the first three changes of W_1. At time $t = 250$ min, the response of this controller is slow, but it achieves its aim. In the disturbance at $t = 450$, the controller considerably decreases its performance and degrades, without reaching the reference. Finally, the PID controller becomes unstable without reaching the reference.

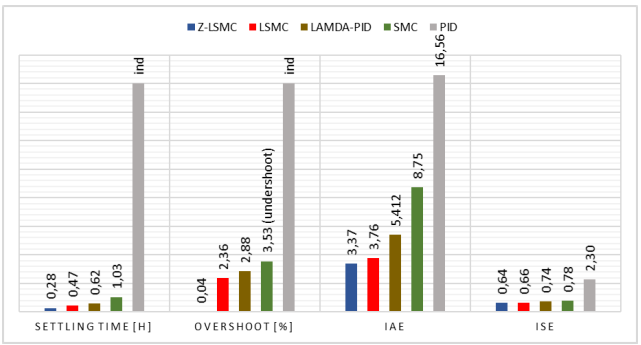

FIGURE 12. Values of the performance indexes of each controller.

From a quantitative point of view, the bars of Fig. 12 presents the values of overshoot, settling time (in a window of 2% of the reference), IAE (Integral Absolute Error) and ISE at time 450 min (the worst condition), to compare the performance of each controller. The IAE index integrates the entire absolute error over time reflecting the cumulative error, and the ISE integrates the square of the error over time in order to penalize the large errors more than the smaller ones. Thus, the controller with the minimum indices performs the best control.

The results in Fig. 11, show that the method with the best performance is Z-LSMC in all the indices. In the case of PID, the controller is unstable, for this reason, its settling time and overshoot are indeterminate (ind), being this the controller with the worst performance. In terms of overshoot, Z-LSMC is considerably the best (0.04%). The ISE and

IAE are consistent with the settling time ($0.28h$) and with the overshoot because they are the minimum, which shows that the error converges to zero faster without the need for a recalibration of the controller, as in the cases of PID and SMC. This is valid to a lesser degree for LSMC and LAMDA-PID.

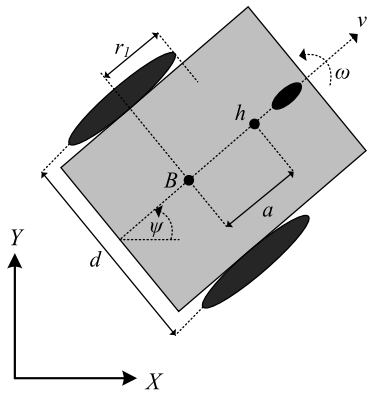

FIGURE 13. Unicycle-like mobile robot parameters.

B. CASE STUDY 2: TRAJECTORY CONTROL OF A MOBILE ROBOT

The complete mathematical representation of the unicycle-like mobile robot involves the kinematic and the dynamic model. For the control of the platform, we implement a cascade scheme with two controllers: to control the kinematic model, is proposed a feedback linearization method based on the robot kinematics, and the dynamic model is controlled with the Z-LSMC and the other proposals, to make the comparative analysis. Fig. 13 shows the robot scheme, with the linear velocity v and angular velocity ω. Besides ψ is the robot orientation, h is the interesting point with r_x, r_y coordinates in the $X-Y$ plane, a is the distance among h and the midpoint B that connects the wheels, and the radius of the wheels is r_1.

1) KINEMATIC CONTROLLER

This controller is designed considering the kinematic model of the robot defined as [61]:

$$\begin{bmatrix} \dot{r}_x(t) \\ \dot{r}_y(t) \\ \dot{\psi}(t) \end{bmatrix} = \begin{bmatrix} cos\psi(t) & -asin\psi(t) \\ sin\psi(t) & acos\psi(t) \\ 0 & 1 \end{bmatrix} \begin{bmatrix} v(t) \\ \omega(t) \end{bmatrix} \tag{73}$$

For the coordinates of the interest point $[r_x, r_y]^T$, the control law is defined as [61]:

$$\begin{bmatrix} v^c_{ref}(t) \\ \omega^c_{ref}(t) \end{bmatrix} = \begin{bmatrix} cos\psi(t) & sin\psi(t) \\ -\frac{1}{a}sin\psi(t) & \frac{1}{a}cos\psi(t) \end{bmatrix} \times \begin{bmatrix} \dot{r}_{xref} + l_x tanh\left(\frac{k_x}{l_x}\tilde{r}_x(t)\right) \\ \dot{r}_{yref} + l_y tanh\left(\frac{k_y}{l_y}\tilde{r}_y(t)\right) \end{bmatrix} \tag{74}$$

where $\tilde{r}_x(t) = r_{xref}(t) - r_x(t)$, and $\tilde{r}_y(t) = r_{yref}(t) - r_y(t)$ are the trajectory errors in the X and Y axis, respectively, k_x and k_y are the gains, $l_x, l_y \in \Re$ are saturation parameters, the $\tanh(\cdot)$ function limits the control action [62], $a > 0$, and $\left[\, v^c_{ref}(t)\ \omega^c_{ref}(t) \,\right]^T$ are the outputs of the kinematic controller [63].

For the stability analysis, it is assumed a perfect velocity tracking $v^c_{ref}(t) \equiv v(t)$ and $\omega^c_{ref}(t) \equiv \omega(t)$. By replacing (74) in (73), it is obtained:

$$\begin{bmatrix} \dot{\tilde{r}}_x \\ \dot{\tilde{r}}_y \end{bmatrix} + \begin{bmatrix} l_x tanh\left(\frac{k_x}{l_x}\tilde{r}_x(t)\right) \\ l_y tanh\left(\frac{k_y}{l_y}\tilde{r}_y(t)\right) \end{bmatrix} = \begin{bmatrix} 0 \\ 0 \end{bmatrix} \tag{75}$$

Let $h(t) = \left[\, r_x(t)\ r_y(t) \,\right]^T$, $\tilde{h}(t) = \left[\, \tilde{r}_x(t)\ \tilde{r}_y(t) \,\right]^T$, then $\dot{\tilde{h}}(t) = \left[\, \dot{\tilde{r}}_x(t)\ \dot{\tilde{r}}_y(t) \,\right]^T$. Thus, (75) is rewritten as:

$$\dot{\tilde{h}}(t) = -\begin{bmatrix} l_x tanh\left(\frac{k_x}{l_x}\tilde{r}_x(t)\right) \\ l_y tanh\left(\frac{k_y}{l_y}\tilde{r}_y(t)\right) \end{bmatrix} \tag{76}$$

In [63], for the kinematic control is proposed the Lyapunov function $V(t) = \frac{1}{2}\tilde{h}^T(t)\,\tilde{h}(t) > 0$, which is positive definite. The Lyapunov function first derivative is:

$$\begin{aligned} \dot{V}(t) &= \frac{1}{2}\tilde{h}^T(t)\,\dot{\tilde{h}}(t) \\ &= -\tilde{r}_x(t)\, l_x tanh\left(\frac{k_x}{l_x}\tilde{r}_x(t)\right) - \tilde{r}_y(t)\, l_y tanh\left(\frac{k_y}{l_y}\tilde{r}_y(t)\right) \end{aligned} \tag{77}$$

Equation (77) is negative definite. Thus, the stability of this controller is guaranteed if: $k_x > 0$, $k_y > 0$, $l_x > 0$ and $l_y > 0$, then $\tilde{h} \to 0$ for $t \to \infty$.

2) DYNAMIC CONTROLLER

For the dynamic controller design, the dynamic model is considered as uncertain. The identification and design of the controller are based on obtaining the approximation of a reduced-order model using the reaction curve method. The dynamic controller receives the linear and angular references, and computes the control actions to reach them. Fig. 14 shows the robot signals when a step input is applied to the linear and angular velocities; these responses look like FOPDT models.

The parameter identification performed for both graphics of Fig. 14 gives the following parameters for the linear speed: $K_v = 1$, $t_{0v} = 0.144\,sec.$, $\tau_v = 0.224 sec.$; and for the angular velocity: $K_\omega = 1, t_{0\omega} = 0.0856 sec$, and $\tau_\omega = 0.116 sec$.

It is important to highlight that the Linear and Angular velocities are independent of each other, as established in [64], which is a characteristic of this type of robot, for which independent Z-LSMC controllers can be used. If they are not independent, the use of decouplers is required, which in this case study is not necessary.

The design process of the Z-LSMC for the linear and angular velocities is similar. In order to summarize the procedure, the linear velocity is detailed as follows.

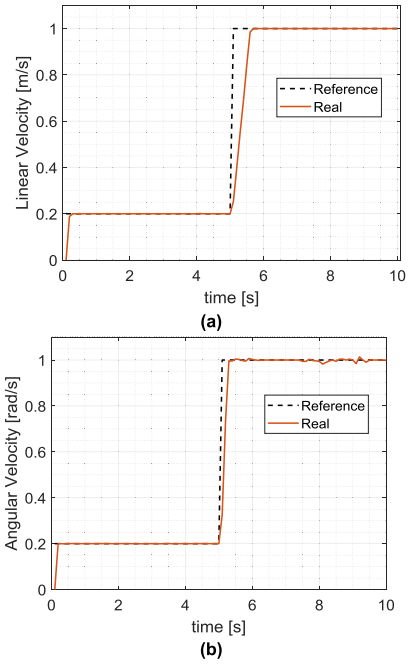

FIGURE 14. Step response of velocity: (a) Linear (b) Angular.

Consider the first order plus dead time for the linear speed with the form of (64):

$$\frac{X_v(s)}{U_v(s)} = \frac{K_v e^{-t_{0v}s}}{\tau_v s + 1} \tag{78}$$

Using the first-order Taylor series approximation for the t_{0v}:

$$e^{-t_{0v}s} \cong \frac{1}{t_{0v}s + 1} (79) \tag{79}$$

Substituting (79) into (78):

$$\frac{X_v(s)}{U_v(s)} \cong \frac{K_v}{(\tau_v s + 1)(t_{0v}s + 1)} = \frac{K_v}{\tau_v t_{0v} s^2 + (\tau_v + t_{0v}) s + 1} \tag{80}$$

Solving (80) in the time domain:

$$\tau_v t_{0v} \ddot{x} + (\tau_v + t_{0v}) \dot{x} + x - K_v u = 0 (81) \tag{81}$$

Rewriting the system in state-space, with $x_1 = x$:

$$\begin{aligned} \dot{x}_1 &= x_2 \\ \dot{x}_2 &= -\frac{(\tau_v + t_{0v})}{\tau_v t_{0v}} x_2 - \frac{1}{\tau_v t_{0v}} x_1 + \frac{K_v}{\tau_v t_{0v}} u \end{aligned} \tag{82}$$

Equation (82) is similar to (27). Then, it is feasible the methodology used to design a stable Z-LSMC as detailed in section II.D.

Observing (82), the linear velocity is second order system ($n = 2$). From (31), $s(t)$ is defined as:

$$\begin{aligned} s(t) &= \left(\frac{d}{dt} + \lambda\right)^2 \int e_v(t)\, dt \\ &= \dot{e}_v(t) + 2\lambda e_v(t) + \lambda^2 \int e_v(t)\, dt \end{aligned} \tag{83}$$

The first derivative of (83) is:

$$\dot{s}(t) = \ddot{e}_v(t) + 2\lambda \dot{e}_v(t) + \lambda^2 e_v(t) = 0 \tag{84}$$

For $n = 2$ in (29):

$$\ddot{e}_v(t) = \dot{x}_{d2}(t) - \dot{x}_2(t) \tag{85}$$

Replacing (82) and (85) in (84) we have:

$$\dot{s}(t) = \dot{x}_{d2}(t) + \frac{(\tau_v + t_{0v})}{\tau_v t_{0v}} x_2 + \frac{1}{\tau_v t_{0v}} x_1 - \frac{K_v}{\tau_v t_{0v}} u + 2\lambda \dot{e}_v(t) + \lambda^2 e_v(t) = 0 \tag{86}$$

The parameter identification has shown that $\frac{K_v}{\tau_v t_{0v}} > 0$, then $b(X, t) > 0$. We use the classes shown in Tables 1 and 2. Fig. 15 presents the classes for u_c. For instance, if $\dot{s}(t) = -0.5$, then the Class 2 is activated ($\gamma_2 = -0.5$) to fulfill $\dot{s}(t) = 0$.

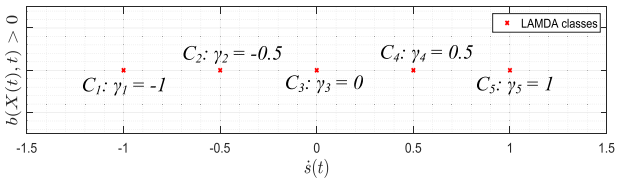

FIGURE 15. Classes and rules for u_c based on $\dot{s}(t)$, for the linear speed of the mobile robot.

Fig. 16 presents the classes for u_d. For instance, if $\dot{s}(t) = 0.5$ and $s(t) = 1$, then the Class 20 is activated ($\gamma_{20} = 1$) to fulfill $s(t)\,\dot{s}(t) < 0$.

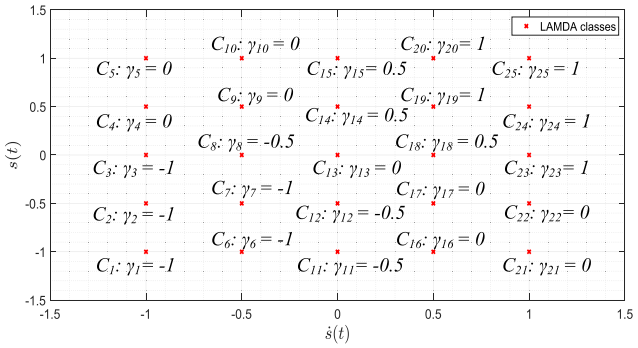

FIGURE 16. Classes and rules for u_d based on $\dot{s}(t)$ and $s(t)$, for the linear velocity of the mobile robot.

The complete control scheme for the trajectory tracking of a mobile robot is presented in Fig. 17, which is tested on a Pioneer 3DX robot [65] running in the Virtual Robot Experimentation Platform "V-REP". This software is used to simulate a robotic environment considering the dynamics and kinematics of the platform [66]. The Z-LSMC has been programmed in Matlab(R) and linked to the V-REP, as shown in Fig. 18. In the environment has been added a disturbance on the floor (unevenness), to test the effectiveness of the controller when the dynamics of the robot changes.

In order to make a comparative analysis, the same controllers defined in subsection IV.A are tested in this experiment, these are: PID, SMC, LAMDA-PID, LSMC, and Z-LSMC. Two trajectories are evaluated, then, it is

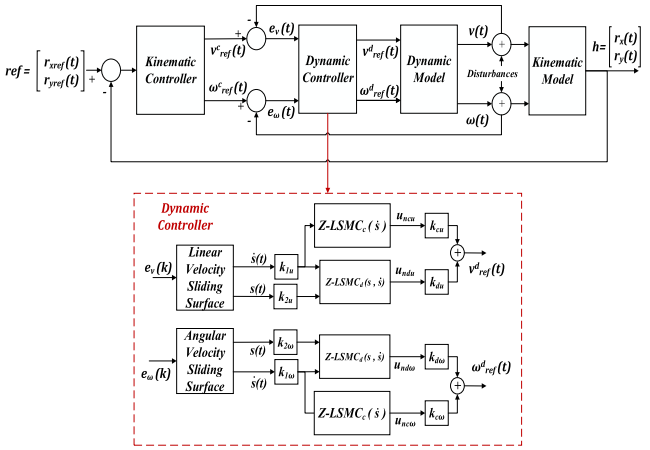

FIGURE 17. Cascade controller for trajectory tracking control.

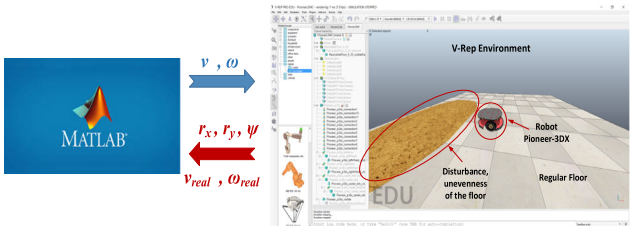

FIGURE 18. V-REP simulation scene showing the Pioneer 3DX robot.

performed a qualitative evaluation through the plot of the response curves, and a quantitative analysis measuring the IAE and ISE performance indices. All the tested controllers have been tuned with the ISE minimization methodology to obtain a fair comparison among them. The tested trajectories are Lenmiscate (see (87)), and Square (see (88)). The initial position of the robot is $r_x = 0m$, $r_y = 0m$.

$$\begin{cases} r_{xref}\ (t) = 1.2\sin(0.063\pi t) \\ r_{yref}\ (t) = 2\sin(0.0315\pi t) \end{cases} \tag{87}$$

$$\begin{cases} r_{xref}\ (t) = 1.5\forall t \in [0,15];\ (4.5-0.2t)\ \forall t \in [15,30]; \\ \quad -1.5\forall t \in [30,45]\,;\ (-10.5+0.2t)\ \forall t \in [45,60] \\ r_{yref}\ (t) = (-1.5+0.2t)\ \forall t \in [0,15];\ 1.5\forall t \in [15,30]; \\ \quad (7.5-0.2t)\ \forall t \in [30,45]\,;\ -1.5\forall t \in [45,60] \end{cases} \tag{88}$$

Figs. 19-24 show the response signals for the linear and angular speeds, trajectory error, and trajectory followed by the robot controlled by the different controllers, to evaluate qualitatively the performance.

The results show that all the controllers perform the trajectory tracking. From a qualitative point of view, it is observed the chattering presented in the controller action of SMC (see Figs. 19b, 20b and 22b), which is the main drawback of this proposal being able to affect the actuators by the oscillations in a real platform. This effect decreases the angular velocity of the square (see Fig. 23b) because the robot follows straight lines. The PID controller has errors in linear and angular velocity (see Figs 19a and 20a), therefore the system does not reach the reference in some instant of time. LAMDA-PID, LSMC and Z-LSMC apparently show nearby results. Particularly, in the square shape, it is noted that Z-LSMC minimizes the deviation between the reference and the real position of the robot, especially at the corners, where abrupt orientation changes occur (see Figs 22e and 23e). The error in both trajectories is around $2cm$, around 1% of relative error when taking into account the radius and the side of the shapes (see Figs. 21 and 24).

Due to the graphic similarity of the responses of the controllers, it is important to do the quantitative analysis based on the IAE and ISE indices, shown in Fig. 25.

The indices displayed in Fig. 25 shows, from the quantitative point of view, that the best controller is Z-LSMC, with the minimum value of IAE and ISE in both trajectories. Especially for the case of square, a figure that has corners in its shape, it is noted that the indices of the Z-LSMC are less than the LSMC. To observe these values, the relative error (RE) is computed:

$$RE_{IAE} = \frac{|IAE_{LSMC} - IAE_{Z-LSMC}|}{IAE_{LSMC}} \times 100\% = 13.6\% \tag{89}$$

$$RSE_{ISE} = \frac{|ISE_{LSMC} - ISE_{Z-LSMC}|}{ISE_{LSMC}} \times 100\% = 6.38\% \tag{90}$$

These values show that Z-LSMC quickly minimizes the error, with respect to the other proposals, reaching the reference faster. The SMC also presents good index values; however, the excessive chattering present in its control action (see Figs 18b, 19b and 21b) can cause heating and decrease the useful life of the actuators in the real robot.

C. COMPUTATIONAL COMPLEXITY

The computational complexity of Z-LSMC is addressed in terms of temporal and spatial complexity The controller is programmed in the software Matlab R2020a, over an Intel (R) Core (TM) i78750H microprocessor @ 2.2GHz.

1) SPATIAL COMPLEXITY

The spatial complexity considers the memory usage and arithmetic complexity, which are computed as follows.

a: MEMORY USAGE

The permanent memory usage contemplates the number of parameters used for the computation of the control action $u(t)$ is based on the number of classes $m = c^l$. For u_c, Z-LSMC uses the descriptor $\dot{s}$, that is, $l = 1$. Thus, the number of parameters to store is $2c$. For u_d, Z-LSMC uses two descriptors s and $\dot{s}$, that is, $l = 2$. Thus, the number of stored parameters is $2c^2$. Besides, are considered the parameters $\sigma_{k,j} = 0.25$, α, λ, three centers, the standard deviation of the reliability, and four scaling gains for calibration. The overall number of parameters stored in memory ($\#stored\_val$) is:

$$\#stored\_val = 2c^2 + 2c + 11 \tag{91}$$

In this paper is assumed that each parameter is stored in 2 bytes of memory [67].

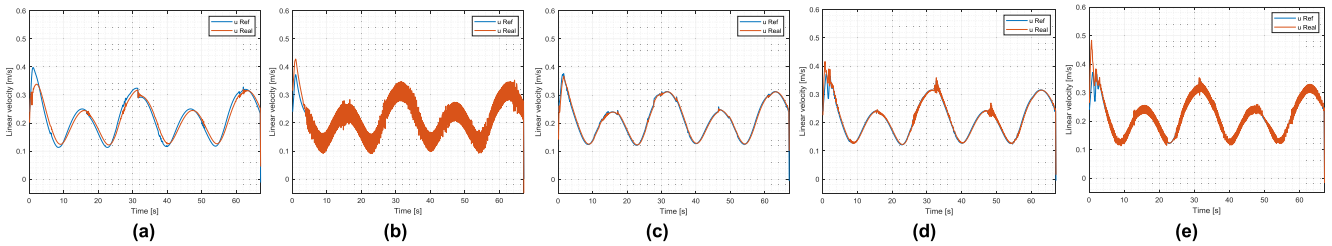

FIGURE 19. Linear speed for the Lenmiscate trajectory (d) LSMC, (e) Z-LSMC.

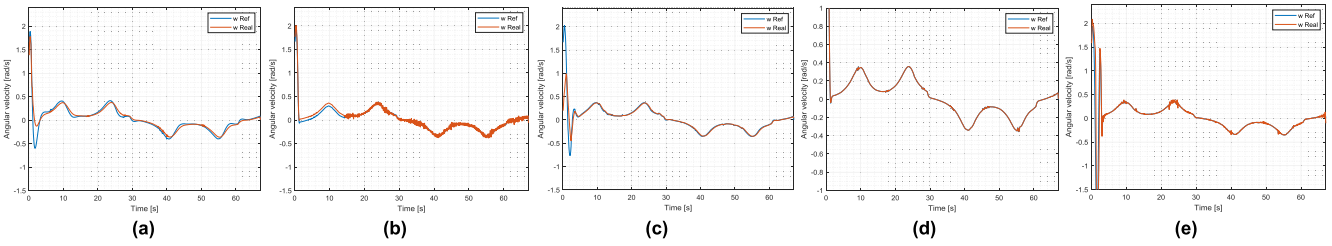

FIGURE 20. Angular speed for the Lenmiscate trajectory followed by the robot: (a) PID, (b) SMC, (c) LAMDA-PID, (d) LSMC, (e) Z-LSMC.

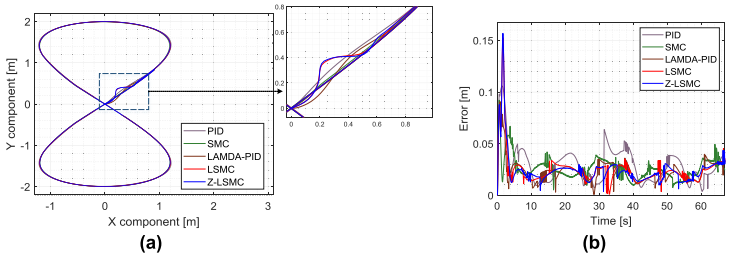

FIGURE 21. (a) Lenmiscate trajectory with the different controllers, (b) trajectory distance error.

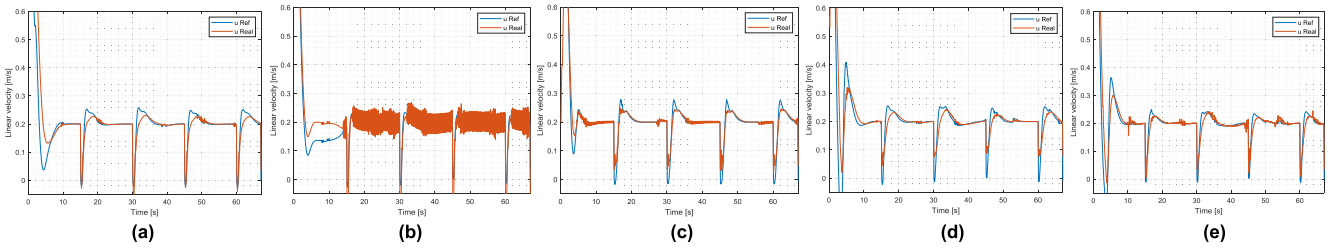

FIGURE 22. Linear speed for the square trajectory followed by the robot: (a) PID, (b) SMC, (c) LAMDA-PID, (d) LSMC, (e) Z-LSMC.

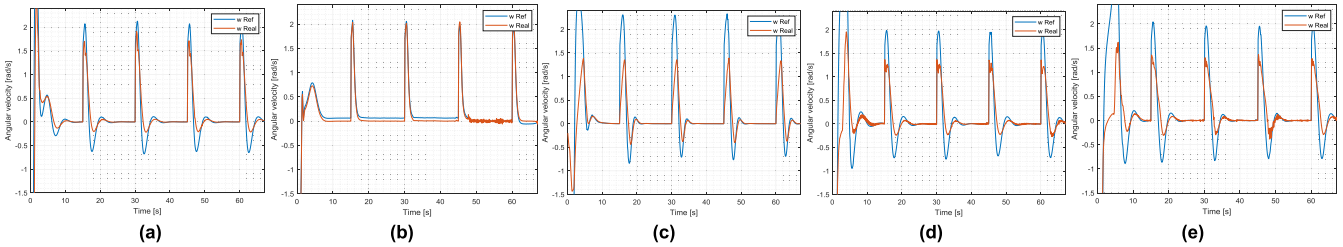

FIGURE 23. Angular speed for the square trajectory followed by the robot: (a) PID, (b) SMC, (c) LAMDA-PID, (d) LSMC, (e) Z-LSMC.

b: NUMBER OF OPERATIONS

The arithmetic complexity is addressed, analyzing the number of arithmetic operations to calculate the control action. The number of operations required to compute the different parameters of the LAMDA controller is presented in Table 4.

The total number of operations shows a quadratic exponent corresponding to the number of classes for each descriptor.

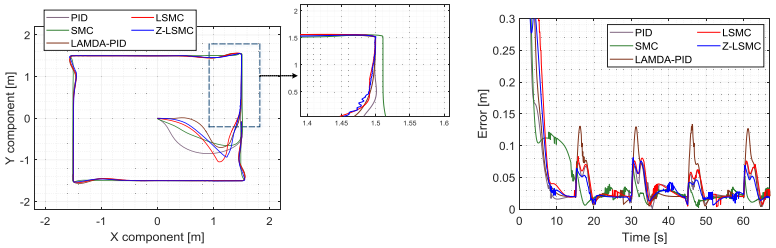

FIGURE 24. (a) Square trajectory with the different controllers, (b) trajectory distance error.

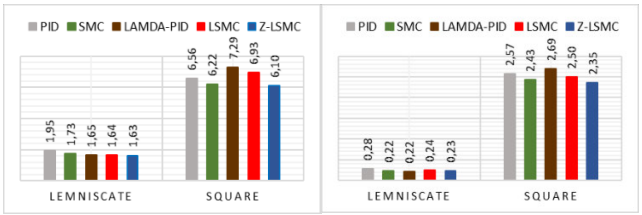

FIGURE 25. Comparative performance indexes of the controllers a) IAE, b) ISE.

TABLE 4. Arithmetic complexity of Z-LSMC.

	u_c	u_d
For $MAD_{k,j}$ (2)	$5c$	$5c^2$
For $GAD_{k,j}$ (6)	$21(c+1)$	$21(c^2+1)$
For Γ, (10)	$2c+1$	$2c^2+1$
For u_c and u_d (11)	$6c+3$	$6c^2+5$
For u, Eq. (21)	1	
Total	$34c^2+34c+53$	

The expression shows the simplicity of the algorithm in the field of spatial complexity.

2) TEMPORAL COMPLEXITY

The temporal complexity allows analyzing the time required in each sample time to calculate the control action. Table 5 presents the average time for 6000 samples, in which the controller output is computed varying the number of classes ''c'' per descriptor.

TABLE 5. Arithmetic complexity of Z-LSMC.

	Number of classes "c"			
	3	5	7	9
u_c	*8.42-6 s*	*9.23e-6 s*	*9.95e-6 s*	*1.17e-5 s*
u_d	*9.41e-5 s*	*1.31e-4 s*	*1.48e-4 s*	*1.66e-4 s*

The values presented in Table 5 demonstrate that the computational time required to compute the controller output of one sample with Z-LSMC is less than 1.7×10^{-4} sec., for the worst case, this is 9 classes per descriptor. Based on these results, the proposed controller can be used in systems that require a sampling greater than that value.

V. CONCLUSION

This paper has formalized a new intelligent controller based on LAMDA, the concepts of SMC, and the Total Utility of Z-numbers, to establish an inference method that improves the performance of the control system. The controller has used the criteria of restriction given for the MADs of LAMDA and the reliability of the measures obtained of the sliding surface and its derivative to compute a more aggressive control action in presence of large errors and smooth control action when the error is close to zero. Besides, one of the foremost qualities of this approach is obtaining a chattering-free robust controller

The Z-LSMC design is simple and only requires to establish the rules for two inputs: the sliding surface and its first derivative. This information is sufficient for the calculation of the overall control action. The Total Utility of Z-numbers is addressed and applied in control systems for the first time in this paper, showing very good results.

The approach has been proven into two case studies with the next control objectives: regulation of a chemical process and trajectory tracking of a mobile robot, to validate our proposal. It is observed that the Z-LSMC controller is capable of reaching the reference quickly and with control actions that would not affect the actuators in a real system since one of its strengths is being robust and chattering-free.

Based on the obtained results, Z-LSMC is the best in terms of performance for the regulation and tracking trajectory objectives presented in the two case studies. Particularly, in the regulation of the chemical process it has been observed that despite the changes in the dynamics of the plant, the controller remains stable and calculates a much smoother control action than the other proposals (see the overshoot), which shows good characteristics with respect to the disturbance rejection. On the other hand, for trajectory tracking, it has been observed that the controller presents very good results, especially it is capable of following the abrupt reference changes faster than the other proposals, without presenting an aggressive control action, as shown the graphics and the indices IAE and ISE.

It should be noted that the main difficulty in the design of the Z-LSMC is the calibration of scaling gains (k_1, k_2, k_c, k_d) since there are no equations formulated for this purpose. An additional drawback is finding the bounds of the functions $(\beta_{dn}, \beta_e, \beta_d, \beta_A)$, however, these can be defined through experimentation and knowledge of an expert regarding the real system. The definition of the centers of the Gaussian functions for reliability is also an open field of investigation since the Z-Numbers and TU are new concepts applied to

control systems; therefore, it is appropriate to deepen the analysis of how this would affect more complex dynamics systems.

As future work, we propose to extend Z-LSMC to Adaptive LAMDA approaches, in which the centers of the classes for the restriction and reliability of the Z-numbers can be automatically computed in online learning mode, in order to avoid the heuristic calibration, which is a time-consuming and complex process in some systems with uncertain dynamics. Furthermore, it is necessary to test the controller in higher-order and unstable systems to evaluate its implementation feasibility to cover a greater number of applications.

REFERENCES

[1] O. Camacho and C. A. Smith, "Sliding mode control: An approach to regulate nonlinear chemical processes," *ISA Trans.*, vol. 39, no. 2, pp. 205–218, Apr. 2000.
[2] Q. H. Ngo and K.-S. Hong, "Adaptive sliding mode control of container cranes," *IET Control Theory Appl.*, vol. 6, no. 5, p. 662, 2012.
[3] A. Shahraz and R. B. Boozarjomehry, "A fuzzy sliding mode control approach for nonlinear chemical processes," *Control Eng. Pract.*, vol. 17, no. 5, pp. 541–550, May 2009.
[4] J. Huang, Z.-H. Guan, T. Matsuno, T. Fukuda, and K. Sekiyama, "Sliding-mode velocity control of mobile-wheeled inverted-pendulum systems," *IEEE Trans. Robot.*, vol. 26, no. 4, pp. 750–758, Aug. 2010.
[5] J. Li and Y. Jinshou, "Nonlinear hybrid adaptive inverse control using neural fuzzy system and its application to CSTR systems," in *Proc. 4th World Congr. Intell. Control Autom.*, vol. 3, 2002, pp. 1896–1900.
[6] J.-J. Wang, "Adaptive inverse position control of switched reluctance motor," *Appl. Soft Comput.*, vol. 60, pp. 48–59, Nov. 2017.
[7] T. P. Nascimento, C. E. T. Dórea, and L. M. G. Gonçalves, "Nonlinear model predictive control for trajectory tracking of nonholonomic mobile robots: A modified approach," *Int. J. Adv. Robotic Syst.*, vol. 15, no. 1, pp. 1–14, 2018.
[8] C. Sun, X. Zhang, Q. Zhou, and Y. Tian, "A model predictive controller with switched tracking error for autonomous vehicle path tracking," *IEEE Access*, vol. 7, pp. 53103–53114, 2019.
[9] R. Wang, J. Bao, and Y. Yao, "A data-centric predictive control approach for nonlinear chemical processes," *Chem. Eng. Res. Design*, vol. 142, pp. 154–164, Feb. 2019.
[10] P. Tatjewski and M. Ławryńczuk, "Algorithms with state estimation in linear and nonlinear model predictive control," *Comput. Chem. Eng.*, vol. 143, Dec. 2020, Art. no. 107065.
[11] Z. Samadikhoshkho, S. Ghorbani, F. Janabi-Sharifi, and K. Zareinia, "Nonlinear control of aerial manipulation systems," *Aerosp. Sci. Technol.*, vol. 104, Sep. 2020, Art. no. 105945.
[12] S. Kim and S. J. Kwon, "Nonlinear optimal control design for under-actuated two-wheeled inverted pendulum mobile platform," *IEEE/ASME Trans. Mechatron.*, vol. 22, no. 6, pp. 2803–2808, Dec. 2017.
[13] S. Rómoli, M. E. Serrano, O. A. Ortiz, J. R. Vega, and G. J. E. Scaglia, "Tracking control of concentration profiles in a fed-batch bioreactor using a linear algebra methodology," *ISA Trans.*, vol. 57, pp. 162–171, Jul. 2015.
[14] A. Rosales, G. Scaglia, V. Mut, and F. di Sciascio, "Formation control and trajectory tracking of mobile robotic systems—A linear algebra approach," *Robotica*, vol. 29, no. 3, pp. 335–349, May 2011.
[15] S. J. Yoo, J. B. Park, and Y. H. Choi, "Indirect adaptive control of nonlinear dynamic systems using self recurrent wavelet neural networks via adaptive learning rates," *Inf. Sci.*, vol. 177, no. 15, pp. 3074–3098, 2007.
[16] G. Jahedi and M. M. Ardehali, "Wavelet based artificial neural network applied for energy efficiency enhancement of decoupled HVAC system," *Energy Convers. Manage.*, vol. 54, no. 1, pp. 47–56, Feb. 2012.
[17] T. Wang, H. Gao, and J. Qiu, "A combined adaptive neural network and nonlinear model predictive control for multirate networked industrial process control," *IEEE Trans. Neural Netw. Learn. Syst.*, vol. 27, no. 2, pp. 416–425, Feb. 2016.
[18] Y. Li, S. Sui, and S. Tong, "Adaptive fuzzy control design for stochastic nonlinear switched systems with arbitrary switchings and unmodeled dynamics," *IEEE Trans. Cybern.*, vol. 47, no. 2, pp. 403–414, Jan. 2016.
[19] R.-E. Precup and H. Hellendoorn, "A survey on industrial applications of fuzzy control," *Comput. Ind.*, vol. 62, no. 3, pp. 213–226, Apr. 2011.
[20] G. Lai, Z. Liu, Y. Zhang, C. L. P. Chen, S. Xie, and Y. Liu, "Fuzzy adaptive inverse compensation method to tracking control of uncertain nonlinear systems with generalized actuator dead zone," *IEEE Trans. Fuzzy Syst.*, vol. 25, no. 1, pp. 191–204, Feb. 2017.
[21] S. Hou, Y. Chu, and J. Fei, "Intelligent global sliding mode control using recurrent feature selection neural network for active power filter," *IEEE Trans. Ind. Electron.*, vol. 68, no. 8, pp. 7320–7329, Aug. 2021.
[22] S. Hou and J. Fei, "A self-organizing global sliding mode control and its application to active power filter," *IEEE Trans. Power Electron.*, vol. 35, no. 7, pp. 7640–7652, Dec. 2020.
[23] G. Feng, "A survey on analysis and design of model-based fuzzy control systems," *IEEE Trans. Fuzzy Syst.*, vol. 14, no. 5, pp. 676–697, Oct. 2006.
[24] L. Teng, Y. Wang, W. Cai, and H. Li, "Robust model predictive control of discrete nonlinear systems with time delays and disturbances via T–S fuzzy approach," *J. Process Control*, vol. 53, pp. 70–79, May 2017.
[25] A. Bayas, I. Škrjanc, and D. Sáez, "Design of fuzzy robust control strategies for a distributed solar collector field," *Appl. Soft Comput.*, vol. 71, pp. 1009–1019, Oct. 2018.
[26] Y.-Q. Ren, X.-G. Duan, H.-X. Li, and C. L. P. Chen, "Multi-variable fuzzy logic control for a class of distributed parameter systems," *J. Process Control*, vol. 23, no. 3, pp. 351–358, Mar. 2013.
[27] T. Niknam and M. H. Khooban, "Fuzzy sliding mode control scheme for a class of non-linear uncertain chaotic systems," *IET Sci., Meas. Technol.*, vol. 7, no. 5, pp. 249–255, Sep. 2013.
[28] M. Roopaei and M. Z. Jahromi, "Chattering-free fuzzy sliding mode control in MIMO uncertain systems," *Nonlinear Anal., Theory, Methods Appl.*, vol. 71, no. 10, pp. 4430–4437, Nov. 2009.
[29] R. Galán, A. Jiménez, R. Sanz, and F. Martía, "Control inteligente," *Intel. Artif.*, vol. 4, no. 10, pp. 43–48, Jul. 2000.
[30] R. H. Abiyev, "Number based fuzzy inference system for dynamic plant control," *Adv. Fuzzy Syst.*, vol. 2016, pp. 1–7, Nov. 2016.
[31] R. H. Abiyev, N. Akkaya, and I. Gunsel, "Control of omnidirectional robot using Z-number-based fuzzy system," *IEEE Trans. Syst., Man, Cybern., Syst.*, vol. 49, no. 1, pp. 238–252, Jan. 2019.
[32] J. Aguilar-Martín and R. L. De Mantaras, "The process of classification and learning the meaning of linguistic descriptors of concepts," in *Approximate Reasoning in Decision Analysis*. Haarlem, The Netherlands: North-Holland, 1982, pp. 165–175.
[33] F. A. Ruiz, C. V. Isaza, A. F. Agudelo, and J. R. Agudelo, "A new criterion to validate and improve the classification process of LAMDA algorithm applied to diesel engines," *Eng. Appl. Artif. Intell.*, vol. 60, pp. 117–127, Apr. 2017.
[34] J. F. B. Valderrama and D. J. L. B. Valderrama, "On LAMDA clustering method based on typicality degree and intuitionistic fuzzy sets," *Expert Syst. Appl.*, vol. 107, pp. 196–221, Oct. 2018.
[35] L. Morales, J. Aguilar, D. Chávez, and C. Isaza, "LAMDA-HAD, an extension to the LAMDA classifier in the context of supervised learning," *Int. J. Inf. Technol. Decis. Making*, vol. 19, no. 1, pp. 283–316, Jan. 2020.
[36] J. C. Atine, A. Doncescu, and J. Aguilar-Martin, "A fuzzy clustering approach for supervision of biological processes by image processing," in *Proc. 4th Conf. Eur. Soc. Fuzzy Log. Technol. (EUSFLAT)*, 2005, pp. 1057–1063.
[37] C. Bedoya, J. W. Villanova, and C. V. I. Narvaez, "Yager–Rybalov Triple ⊓ operator as a means of reducing the number of generated clusters in unsupervised anuran vocalization recognition," in *Proc. Mexican Int. Conf. Artif. Intell.*, 2014, pp. 382–391.
[38] L. Morales, C. A. Ouedraogo, J. Aguilar, C. Chassot, S. Medjiah, and K. Drira, "Experimental comparison of the diagnostic capabilities of classification and clustering algorithms for the QoS management in an autonomic IoT platform," *Service Oriented Comput. Appl.*, vol. 13, no. 3, pp. 199–219, Sep. 2019.
[39] L. Morales, J. Aguilar, A. Rosales, J. A. G. D. Mesa, and D. Chavez, "An intelligent controller based on LAMDA," in *Proc. IEEE 4th Colombian Conf. Autom. Control (CCAC)*, Oct. 2019, pp. 1–6.
[40] L. Morales-Escobar, J. Aguilar, A. Garcés-Jiménez, J. A. G. De Mesa, and J. M. Gomez-Pulido, "Advanced fuzzy-logic-based context-driven control for HVAC management systems in buildings," *IEEE Access*, vol. 8, pp. 16111–16126, 2020.
[41] L. Morales, J. Aguilar, A. Rosales, D. Chávez, and P. Leica, "Modeling and control of nonlinear systems using an adaptive LAMDA approach," *Appl. Soft Comput.*, vol. 95, Oct. 2020, Art. no. 106571.

[42] L. Morales, D. Pozo, J. Aguilar, and A. Rosales, "Adaptive LAMDA applied to identify and regulate a process with variable dead time," in *Proc. IEEE Int. Conf. Fuzzy Syst. (FUZZ-IEEE)*, Jul. 2020, pp. 1–8.
[43] L. Morales, J. Aguilar, O. Camacho, and A. Rosales, "An intelligent sliding mode controller based on LAMDA for a class of SISO uncertain systems," *Inf. Sci.*, vol. 567, pp. 75–99, Aug. 2021.
[44] L. A. Zadeh, "A note on Z-numbers," *Inf. Sci.*, vol. 181, no. 14, pp. 2923–2932, Jul. 2011.
[45] R. A. Aliev, W. Pedrycz, O. H. Huseynov, and S. Z. Eyupoglu, "Approximate reasoning on a basis of Z-number-valued if–then rules," *IEEE Trans. Fuzzy Syst.*, vol. 25, no. 6, pp. 1589–1600, Dec. 2017.
[46] B. Kang, D. Wei, Y. Li, and Y. Deng, "A method of converting Z-number to classical fuzzy number," *J. Inf. Comput. Sci.*, vol. 9, no. 3, pp. 703–709, 2012.
[47] R. A. Aliev, A. V. Alizadeh, and O. H. Huseynov, "The arithmetic of discrete Z-numbers," *Inf. Sci.*, vol. 290, pp. 134–155, Jan. 2015.
[48] R. A. Aliev and L. M. Zeinalova, "Decision making under Z-information," *Stud. Comput. Intell.*, vol. 502, pp. 233–252, Nov. 2014.
[49] B. Kang, D. Wei, and Y. Li, "Decision making using Z-numbers under uncertain environment," *J. Comput. Inf. Syst.*, vol. 8, no. 7, pp. 2807–2814, 2012.
[50] H.-G. Peng and J.-Q. Wang, "Outranking decision-making method with Z-number cognitive information," *Cognit. Comput.*, vol. 10, no. 5, pp. 752–768, Oct. 2018.
[51] Z. Tao, X. Liu, H. Chen, J. Liu, and F. Guan, "Linguistic Z-number fuzzy soft sets and its application on multiple attribute group decision making problems," *Int. J. Intell. Syst.*, vol. 35, no. 1, pp. 105–124, Jan. 2020.
[52] W. Jiang, C. Xie, B. Wei, and Y. Tang, "Failure mode and effects analysis based on Z-numbers," *Intell. Automat. Soft Comput.*, vol. 24, no. 1, pp. 1–8, May 2018.
[53] B. Kang, Y. Deng, and R. Sadiq, "Total utility of Z-number," *Int. J. Speech Technol.*, vol. 48, no. 3, pp. 703–729, Mar. 2018.
[54] R. H. Abiyev, I. Günsel, and N. Akkaya, "Z-number based fuzzy system for control of omnidirectional robot," in *Intelligent Technologies and Robotics*. Cham, Switzerland: Springer, 2019.
[55] M. E. Shalabi, H. El-Hussieny, A. A. Abouelsoud, and A. M. R. F. Elbab, "Control of automotive air-spring suspension system using Z-number based fuzzy system," in *Proc. IEEE Int. Conf. Robot. Biomimetics (ROBIO)*, Dec. 2019, pp. 1306–1311.
[56] M. Abdelwahab, V. Parque, A. M. R. F. Elbab, A. A. Abouelsoud, and S. Sugano, "Trajectory tracking of wheeled mobile robots using Z-number based fuzzy logic," *IEEE Access*, vol. 8, pp. 18426–18441, 2020.
[57] T. Takagi and M. Sugeno, "Fuzzy identification of systems and its applications to modeling and control," *IEEE Trans. Syst., Man, Cybern.*, vol. SMC-15, no. 1, pp. 116–132, Jan./Feb. 1985.
[58] J.-J. Slotine and W. Li, *Applied NoLinear Optimal Control*. Upper Saddle River, NJ, USA: Prentice-Hall, 1991.
[59] H.-T. Yau and C.-L. Chen, "Chattering-free fuzzy sliding-mode control strategy for uncertain chaotic systems," *Chaos, Solitons Fractals*, vol. 30, no. 3, pp. 709–718, Nov. 2006.
[60] E. Iglesias, Y. García, M. Sanjuan, O. Camacho, and C. Smith, "Fuzzy surface-based sliding mode control," *ISA Trans.*, vol. 46, no. 1, pp. 73–83, Feb. 2007.
[61] F. G. Rossomando, C. Soria, and R. Carelli, "Sliding mode neuro adaptive control in trajectory tracking for mobile robots," *J. Intell. Robotic Syst.*, vol. 74, nos. 3–4, pp. 931–944, Jun. 2014.
[62] F. G. Rossomando and C. M. Soria, "Identification and control of nonlinear dynamics of a mobile robot in discrete time using an adaptive technique based on neural PID," *Neural Comput. Appl.*, vol. 26, no. 5, pp. 1179–1191, Jul. 2015.
[63] F. G. Rossomando, C. Soria, and R. Carelli, "Autonomous mobile robots navigation using RBF neural compensator," *Control Eng. Pract.*, vol. 19, no. 3, pp. 215–222, Mar. 2011.
[64] G. Scaglia, J. Guevara, A. Rosales, L. Guevara, and O. Camacho, "A linear algebra controller based on reduced order models applied to trajectory tracking for mobile robots: An experimental validation," *Int. J. Autom. Control*, vol. 13, no. 2, p. 176, 2019.
[65] *Pioneer 3-DX*, Adept Technol., 2011.
[66] E. Rohmer, S. P. N. Singh, and M. Freese, "V-REP: A versatile and scalable robot simulation framework," in *Proc. IEEE/RSJ Int. Conf. Intell. Robots Syst.*, Nov. 2013, pp. 1321–1326.
[67] Y. H. Kim, S. C. Ahn, and W. H. Kwon, "Computational complexity of general fuzzy logic control and its simplification for a loop controller," *Fuzzy Sets Syst.*, vol. 111, no. 2, pp. 215–224, Apr. 2000.

L. MORALES received the degree in electronics and control engineering from the Escuela Politécnica Nacional, Quito, Ecuador, in 2010, and the M.Sc. degree in automatic and robotics from the Universitat Politécnica of Catalunya, Spain, in 2012. He is currently pursuing the Ph.D. degree in the field of control systems with the Escuela Politécnica Nacional. He is also an Assistant Professor with the Escuela Politécnica Nacional, where he has taught electronics and automation engineering degree. His research interests include automatic systems and artificial intelligence applied to control systems.

J. AGUILAR (Member, IEEE) received the M.Sc. degree in computer science from Université Paul Sabatier, France, in 1991, and the Ph.D. degree in computer science from Université Rene Descartes, France, in 1995. He has completed the postdoctoral studies with the Department of Computer Science, University of Houston, from 1999 to 2000, and the Laboratoire d'analyse et d'architecture des systèmes (LAAS), CNRS, Toulouse, France, from 2010 to 2011.

He received the title of a Systems Engineer from the Universidad de los Andes, Venezuela, in 1987. He is currently a Full Professor with the CEMISID, Escuela de Ingeniería de Sistemas, Universidad de Los Andes, Mérida, Venezuela. He has published more than 500 articles and ten books in the field of parallel and distributed computing, computer intelligence, and science and technology management. His research interests include artificial intelligence, semantic mining, big data, emerging computing, and intelligent environments. He is a member of Mérida Science Academy and the IEEE CIS Technical Committee on Neural Networks.

A. ROSALES (Senior Member, IEEE) received the Ph.D. degree in control systems engineering from the Universidad Nacional de San Juan, Argentina. He is currently an Engineer in electronics and control with the Escuela Politécnica Nacional (EPN), Ecuador, and an Invited Researcher with the Universidad de Hannover, Germany. He has been the Director of the Doctorate Program in electrical engineering, EPN, since 2018, and the Representative of the Professors with the Polytechnic Council, from 2018 to 2021. He holds the position of a Senior Lecturer with the Department of Automation and Industrial Control, EPN. His research interests include robotic systems, industrial process control, advanced control, precision agriculture, biomechanical systems, and cooperative systems. He was the Founder and the First President (Chair) of the IEEE Robotics and Automation Society (RAS), Ecuador Chapter. He was the Director of Research and Social Projection of the EPN, in 2015 and 2017, the General Technical Coordinator of CEAACES, in 2014, the General Coordinator and the Research Coordinator of the Ecuadorian Network of Universities and Polytechnic Schools—REDU, from 2012 to 2013, the First Secretary of the Embassy of Ecuador, Spain, in 2016, and an Editor of the *Polytechnic Journal*, from 2012 to 2013.

D. POZO-ESPIN received the degree in electronics and control engineering from the Escuela Politécnica Nacional, Quito, Ecuador, in 2010, and the M.Sc. degree in automatic and robotics from the Universitat Politécnica de Catalunya, Spain, in 2012. He worked in automation and control area with the Escuela Politécnica Nacional as a full-time Adjunct Lecturer, from 2010 to 2011, and an Assistant Lecturer, from 2013 to 2014. He currently works as a Professor with the Universidad de Las Américas, Quito. His main research interests include robotics, and machine learning and control.